1997

Selection and development of a miniature bioaerosol sampler

Jason Bradley Taylor
San Jose State University

INFORMATION TO USERS

This manuscript has been reproduced from the microfilm master. UMI films the text directly from the original or copy submitted. Thus, some thesis and dissertation copies are in typewriter face, while others may be from any type of computer printer.

The quality of this reproduction is dependent upon the quality of the copy submitted. Broken or indistinct print, colored or poor quality illustrations and photographs, print bleedthrough, substandard margins, and improper alignment can adversely affect reproduction.

In the unlikely event that the author did not send UMI a complete manuscript and there are missing pages, these will be noted. Also, if unauthorized copyright material had to be removed, a note will indicate the deletion.

Oversize materials (e.g., maps, drawings, charts) are reproduced by sectioning the original, beginning at the upper left-hand corner and continuing from left to right in equal sections with small overlaps. Each original is also photographed in one exposure and is included in reduced form at the back of the book.

Photographs included in the original manuscript have been reproduced xerographically in this copy. Higher quality 6" x 9" black and white photographic prints are available for any photographs or illustrations appearing in this copy for an additional charge. Contact UMI directly to order.

UMI

A Bell & Howell Information Company
300 North Zeeb Road, Ann Arbor MI 48106-1346 USA
313/761-4700 800/521-0600

SELECTION AND DEVELOPMENT OF A MINIATURE BIOAEROSOL SAMPLER

A Thesis
Presented to
The Faculty of the Department of Chemical Engineering
San Jose State University

In Partial Fulfillment
of the Requirements for the Degree
Master of Science

by
Jason Bradley Taylor

May, 1997

Thesis approved for the Department of Chemical Engineering

Melanie McNeil Date 4-11-97

Dr. M. A. McNeil, Thesis Advisor and Chairperson
SJSU, Department of Chemical Engineering

Lark V. Schneider Date 4/11/97

Dr. L. V. Schneider, Reading Committee Member
SRI International

Patrick Hamill Date 4-11-97

Dr. P. Hamill, Reading Committee Member
SJSU, Department of Physics

APPROVED FOR THE UNIVERSITY

M. Lou Salwasser Date 4/19/97

ABSTRACT

SELECTION AND DEVELOPMENT OF A MINIATURE BIOAEROSOL SAMPLER

By Jason B. Taylor

Aerosol samplers have long been used for the purpose of detecting and characterizing airborne particulates. Bioaerosol sampling includes two interdependent operations: the collection of airborne particles, which is governed by aerosol physics, and the assay of microorganisms within the sample, which is governed by microbiology. Recent advances in analytical detection methods have provided the ability for real-time, single-agent detection, and hence have reduced the sample size needed, and as a result, the type of samplers required. This thesis investigated the feasibility of using a miniature cyclone and a miniature electrostatic precipitator to collect aerosols of *Bacillus subtilis* and *Serratia marcescens*. The physical and bioefficiencies of each device were determined at 5, 15, and 25 liters per minute. It was found that both samplers achieved bioefficiency levels of near 100% for both microorganisms, while the electrostatic precipitator achieved an average 30% increase in physical efficiency over the cyclone for both microorganisms.

Acknowledgments

I wish to thank Dr. L. V. Schneider and SRI International for the opportunity to develop this thesis work, in cooperation with San Jose State University. My thanks also go to Dr. K. Mortelmans for microbiological assistance and analysis, as well as Dr. M.A. McNeil and Dr. P. Hamill for their guidance and reviews. I would not have been able to complete this work without the persistence and patience of my wife Jacki. I also acknowledge my two children, Kaitlyn and Andrew, without whose help this work could have been completed in half the time.

Table Of Contents

	Page
List of Figures	viii
List of Tables	ix
Chapter 1. Introduction	1
1.1 Sampler Selection in General	4
1.2 Sampler Criteria	6
1.3 Collection Mechanisms	7
1.4 Sampler Evaluation	17
Chapter 2. Literature Review	19
2.1 Sampler Selection	20
Chapter 3. Hypothesis	32
Chapter 4. Materials and Methods	33
4.1 Equipment	33
4.2 Microorganisms	36
4.3 Determination of Physical Efficiency	38
4.4 Determination of Bioefficiency	41
4.5 Aerosol Size Distributions	45
Chapter 5. Experimental Results	48
5.1 Aerosol Size Distribution Data	48
5.2 Cyclone Physical Efficiency Data	55
5.3 Electrostatic Precipitator Physical Efficiency Data	55
5.4 Cyclone Bioefficiency Data	58
5.5 Electrostatic Precipitator Bioefficiency Data	59
5.6 Power Requirement Data	62
Chapter 6. Discussion	64
Chapter 7. Conclusions	71

Table Of Contents (cont.)

References	72
Appendix A. Variable definitions for Table 1	75
Appendix B. Results of a Comparison: 10-mm Cyclone and a Comparably Sized ESP	76
Appendix C. Method for determining mass median diameter and GSD using a weighted curve fit	77
Appendix D. Tables of Experimental Data	79
Appendix E. Plots of Experimental Data	92

List of Figures

	Page
Figure 1. Schematic of a typical cyclone.	21
Figure 2. Collection efficiencies of several miniature cyclones.	24
Figure 3. Collection efficiency of a 10-mm cyclone.	26
Figure 4. Schematic of an electrostatic precipitator.	29
Figure 5. Apparatus for bioaerosol generation and collection.	35
Figure 6. MMDs of *B. subtilis* and *S. marcescens*.	49
Figure 7. Particle Size Distributions of *B. subtilis*.	50
Figure 8. Particle Size Distributions of *S. marcescens*.	51
Figure 9. Plot to determine cumulative fractions for *S. marcescens*.	53
Figure 10. Effective cutoff diameters.	54
Figure 11. Cyclone and ESP physical efficiencies.	57
Figure 12. Cyclone and ESP bioefficiencies.	61
Figure 13. Comparison of power requirements for the cyclone and ESP.	63

List of Tables

	Page
Table 1. Summary of mechanisms and parameters in aerosol deposition.	9
Table 2. Experiments for physical and bioefficiency measurements.	44
Table 3. Equipment and material summary.	47

Chapter 1. Introduction

Aerosol samplers have long been used for the purpose of detecting and characterizing airborne particulates. The primary motivation for aerosol monitoring is the enormous amount of loss in human lives and health, as well as the major economic impact due to respiratory infection from aerosol inhalation, airborne plant and animal diseases, and other pollutants.[1] In addition, the ever-increasing threat of biological weapons has provided a strong incentive to develop better and smaller bioaerosol sampling systems, and to continue making improvements in our ability to detect ever smaller quantities of bioaerosols.

The term "aerosol" applies to solid or liquid particulates suspended in air or other gaseous environments. These particles range in size, shape, and origin, and are as varied as matter itself. A special class of aerosols is comprised of particles of biological origin or activity, and include bacterial cells, viruses, pollen, spores, toxins, etc. These "bioaerosols" represent a diverse and complex variety of sizes and types, ranging from viruses (0.015-0.45 μm) to fungal spores (1.0-100 μm).[2] The complexity of sampling and characterizing these bioaerosols is enhanced by their frequent occurrence in aggregates or their attachment to non-viable particles, such as dust or fog droplets. Bioaerosol sampling includes two interdependent operations: the

collection of airborne particles, which is governed by aerosol physics, and the assay of microorganisms within the sample, which is governed by microbiology.

Bioaerosols pose several possible hazards to living things, including infectivity, allergenicity, pharmacological activity, and toxicity. Particles in the respirable range, from 1-5 μm, are of particular concern, as these may be taken into the deep lung, and are typical of particles generated in the workplace, by biological weapons, etc. Particles larger than 10 μm in diameter are deposited mostly in the throat and nasal passage, while those that are 3-5 μm deposit mostly in the bronchi. Particles that are 2 μm and smaller can penetrate efficiently into the lower lung and alveoli, while those less than about 0.5 μm do not efficiently deposit in the lung, and are usually exhaled relatively easily.[3]

Despite the fact that bioaerosol monitoring has wide application and important health and environmental implications, there are currently no standard protocols for sampling airborne microorganisms, and no occupational exposure limits for airborne microorganisms have been set.[4] In addition, very few samplers have been fully characterized in terms of bioefficiency, which is a measure of how well the sampler maintains the viability of the sampled bioaerosol. Henningson and Ahlberg[4] attribute the

lack of scientific progress in the field of bioaerosol sampling over the past several decades to non-standardized test methods and procedures.

The methods of analysis available for characterization of the sampled bioaerosol also impose restrictions on the type of sampler used, and its subsequent accuracy in detection and identification. Recent advances in analytical detection methods (e.g., PCR amplification and upconverting phosphor immunoassays) have provided the ability for real-time, single-agent detection, and hence have reduced the sample size needed, and as a result, the type of sampler required. It is therefore desirable to develop a sampler to couple with these new detection technologies, and create a miniaturized, low-power sampler for use in the detection of bioaerosols. The requirement for low power is necessary for remote field sampling applications, where there are no power outlets, as well as to keep the unit as physically small as possible.

The selection and development of an aerosol collection device for use as a miniaturized, real-time, low-power, and highly sensitive bioaerosol sampler is the subject of this thesis.

1.1 Sampler Selection in General

The choice of a sampler used to collect an aerosol depends on a number of factors.[4] These include: location (indoor or outdoor), specificity (whether one species needs to be detected against a background of others), level of sensitivity required (dependent on the microorganism and its hazardous concentration threshold), speed with which a result is needed (dependent on the implication of the result), and the particle size of interest (i.e., respirable fraction only). In addition to these factors, bioaerosols must be collected with minimal damage to ensure their viability for detection, if the method of identification requires it. Shear forces and desiccation, for example, may damage microbiological materials in a manner that leads to false negative detection. Indeed, the overall performance of a bioaerosol sampler may be divided into two areas: (1) the *physical efficiency*, which is concerned with obtaining a complete and representative sample of the aerosol, and (2) the *bioefficiency*, which involves the minimizing of damage to the particles by the sampling process, thus retaining their viability. Maximizing both of these parameters is challenging, as an improvement in the physical collection efficiency is often countered by a decrease in bioefficiency, and *vice versa*. The physical efficiencies of bioaerosol samplers can be well characterized using current methods, and the collection of a representative sample is important in the analysis and extrapolation of the

test results. The bioefficiency, however, is difficult to determine completely. This is due to the inherent limitations in sampling and analysis, and differentiating how many of the microorganisms have been killed by collection and by assaying, or in the airborne state prior to sampling. The true number of microorganisms in the aerosol may thus be significantly higher than the number of microorganisms in the analyzed sample. This makes the evaluation of sampler effectiveness in maintaining bioefficiency more difficult than the determination of physical efficiency. The bioefficiency may or may not be a critical factor, however, depending on the target microorganism and the analytical method used. Many microorganisms can produce a toxic response or allergic reaction whether they are viable or not, as the dead cells and cell debris may provoke the same response as the viable cells. In these situations, the total number of airborne cells is the critical factor. Moreover, some analytical techniques, such as immunoassay methods, cannot distinguish between viable and non-viable cells. A high bioefficiency may still be desired from a sampler, however, because it may be necessary to collect samples for further analysis, or to verify identification by alternate methods.

In addition to the physical sampling method, the type of analysis must also be considered in bioaerosol sampler selection. The choice will be based on the type of agents that are of interest, any necessary preparation steps

required prior to detection (e.g., DNA isolation and amplification), and compatibility with the detection probes and labels. There are currently at least five major methods of sample analysis: culture (growth of microorganisms), direct microscopy, bioassay (PCR), biochemical assay (e.g., ATP-bioluminescence), and immunological assay.[6] Each analytical method places different requirements on the collection mechanism and the type of collection medium employed. In addition, the nature of the analyte (i.e., biotoxin, live, or dormant) places different requirements on the collection system.

1.2 Sampler Criteria

Due to the complexity of bioaerosols and varied environmental conditions, no one sampler or single-step sampling procedure can realistically be used to characterize all of the organisms in a sampled volume of air. Samplers must therefore be chosen or designed with relatively narrow sampling criteria, to be used for a specific organism, or range of organisms, and operating conditions. For the selection of an appropriate sampler to be integrated into a miniature bioaerosol sampling and detection system using recent advances in immuno and nucleic acid detection methods, a number of criteria must be met. These are:

- The sampler must be able to collect the particles of interest (i.e., the respirable fraction from 1- 5 μm), and collect them into a liquid for immediate use in the detection system.
- The sampler must be able to be scaled down to take advantage of the miniature size and weight characteristics made possible with the new generation of detection systems, and therefore find application as a small, completely integrated, and stand-alone point detection system.
- The sampler must achieve acceptable levels of both physical and bioefficiency.

1.3 Collection Mechanisms

To design or select an appropriate sampler to meet these criteria and be used in a miniature biosensor detection system, it is necessary to understand the mechanisms that are used in aerosol and bioaerosol collection. These mechanisms have a direct impact on the choice of sampler for a given target organism and environmental conditions, as well as the subsequent analysis and the overall sampling effectiveness. It is also important to understand how these mechanisms scale with the size of the particle to be collected, which is a key factor in determining a suitable collection device for use in a miniature detection system.

Aerosols are collected by utilizing various physical forces to separate particles from an air stream. These forces may be conveniently used to classify the samplers and techniques used in aerosol collection. Lunde and Lapple[8] list the following six aerosol sampling mechanisms, along with the type of physical gradient that causes separation: (1) flow-line interception (physical gradient); (2) inertial deposition (velocity gradient); (3) diffusional deposition (concentration gradient); (4) gravity settling (elevation gradient); (5) electrostatic precipitation (electric field gradient); and (6) thermal precipitation (temperature gradient). Table 1 lists these mechanisms, along with the corresponding force gradient and governing dimensionless parameter. Variables for Table 1 are defined in Appendix A.

Table 1. Summary of mechanisms and parameters in aerosol deposition.

Deposition	Origin of Force Field	Basic Parameter	Force Equation
Flow-line interception	Physical gradient	$N_{sf} = \left(\frac{D_p}{D_b}\right)$	
Inertial deposition	Velocity gradient	$N_{st} = \left(\frac{K_m \rho_s D_p^2 V_o}{18 \mu D_b}\right)$	$F = \pi a \rho_p D_p^3 / 6$
Diffusional deposition	Concentration gradient	$N_{sd} = \left(\frac{D_v}{V_o D_b}\right)$	$F = kT / L_m$
Gravity settling	Elevation gradient	$N_{sg} = \left(\frac{u_t}{V_o}\right)$	$F = \frac{\pi g \rho_p D_p^3 (\rho_p - \rho)}{6}$
Electrostatic precipitation	Electric-field gradient		$F = \frac{\pi \underline{\varepsilon} \delta E_{ps}^2 D_p^2}{4(L / D_p)^2}$
	a. Attraction	$N_{sec} = \left(\frac{K_m Q_p \varepsilon_b}{\mu D_p V_o}\right)$	
	b. Induction	$N_{sei} = \left(\frac{\delta_p - 1}{\delta_p + 2}\right)\left(\frac{K_m D_p^2 \delta_o \varepsilon_b 2}{\mu D_b V_o}\right)$	
Thermal precipitation	Temperature gradient	$N_{st} = \left(\frac{T - T_b}{T}\right)\left(\frac{\mu}{K_m \rho D_b V_o}\right)\left(\frac{k_t}{2k_t + k_{tp}}\right)$	

All sampling devices use one or more of these forces, with the most common for bioaerosol sampling being inertial deposition. Several reviewers[4,5,7] classify the major types of bioaerosol sampling devices by their physical mechanism. These may be classified as follows: (1) impaction onto a solid or semi-solid surface, (2) impingement into a liquid, (3) collection onto a porous material, and (4) other devices (i.e., electrostatic and thermal precipitators). By a simple examination of these collection mechanisms, and the types of samplers that utilize them, a sampling strategy can be selected that would most nearly satisfy the criteria for our miniature detection system.

Gravity settling represents the simplest form of collection, and requires little training and minimal equipment. This mechanism has been used extensively with microbial settling plates. Results are qualitative only, however, and no information can be extracted on the volume of air from which the particles have been sampled. The collection efficiency of a settling plate also depends on the particle size as well as the changing levels of atmospheric motion.[6] Settling plates, because of this relationship, are biased towards collecting larger particles, and are subject to a large variation in collection efficiency.[4] This method has, however, been used frequently as a

reference in some studies, even though it is non-quantitative and highly variable.

Flow-line interception is a theoretical situation involving a hypothetical particle having finite size but no mass and following a streamline around a collection body. If the particle gets physically close enough to the collection body (i.e., one particle diameter), the particle may be collected. This mechanism does not consider inertial or Brownian diffusion, but merely describes the physical boundary condition imposed on the path of a particle, and hence is combined with other forces in the collection of particles. Filters are the practical example of this mechanism.

Collection by filtration is a widely used method because of its simplicity and low cost. Recovery of the sample from the filter may be difficult, however, and not very reproducible. In addition, filtration for air sampling of bioaerosols may cause desiccation due to the sampled air passing over the deposited particles, and hence may destroy viability of some organisms. Filters also require a relatively large vacuum source to overcome increasing pressure drop across the filter medium due to the build-up of particulates.

Inertial Deposition is the most common mechanism in aerosol sampling and represents the widest variety of samplers. Samplers that

utilize this principle have been used extensively for many years because of their simplicity and effectiveness, including some devices that can classify particles into distinct size ranges (e.g., cascade impactors), based on simple and relatively accurate theoretical design parameters. Size-fractionating impactors such as the Anderson microbial impactor provide valuable information on the particle size distribution supporting microbial cells, and hence their potential for penetration due to inhalation.[9] Inertial impactors operate under the principle that if a fluid stream is directed towards a surface at high velocity, and subsequently forced to change direction, particles of sufficient inertia (determined by the product of mass and velocity) will impact on the surface, while those with less inertia will follow the streamline around the surface and not be collected. Inertial samplers, therefore, are directly dependent on the mass of the particles, and an increase or decrease in particle mass will affect the collection efficiency much more than samplers that utilize non-inertial mechanisms.

Inertial impactors may be further classified by the type of collecting surface: solid, semi-solid, or liquid (impingers). Many microbiological samplers make use of nutrient agar plates (semi-solid surfaces) as the collection surface. This allows direct detection of microorganisms based on the growth of colonies on the plates. Growth typically takes 1-7 days,

however, as well as controlled laboratory conditions. Other devices, such as Spore Traps, Rotorod, RCS, and STA samplers make use of adhesive solid or semi-solid surfaces to trap particles and provide a convenient method for analysis. Subsequent incubation to develop the colonies from impacted microbial cells, or direct counting from microscopic analysis, is generally straightforward, but relatively time-intensive. Solid surface samplers also require operator intervention, which is not conducive to stand-alone point detection applications.

Samplers in which a liquid is used as the collection medium are typically referred to as impingers. In these devices, the aerosol is drawn through a body of liquid, and the particles are collected by impingement with the liquid. The viability of collected cells may be affected by the velocity of the particles as they impact the liquid, where higher velocities would create higher shear forces on the particles. Collecting the sample into a liquid is desirable for many of the newer types of detection systems, however, because it makes subsequent immuno and biochemical assaying relatively simple. The most widely used impinger is the Porton Raised Impinger (AGI-30 or the AGI-4), which uses a critical flow orifice to control the inlet flow rate, and has an inlet designed to simulate the human nasal passage by separating larger particles from the air stream.

Cyclones are also widely used inertial impactors. The principle of collection involves forcing the aerosol sample into centrifugal motion, and particles with sufficient inertia will leave the air stream and impact on the walls of the cyclone. Though they may be used dry, cyclone samplers for bioaerosols are frequently used with a liquid which is continuously introduced through a spray nozzle at the sample inlet. The liquid prevents desiccation, serves to wash deposited particles from the walls into the collection vessel at the bottom of the sampler, and, since the particles are moistened while still in the air stream, simulates to some degree the deposition inside a mammalian breathing tract.[9] Moreover, the physical collection efficiency of a cyclone has been shown to increase when a cyclone was used with a liquid,[10] possibly because the fine mist sprayed into the inlet of the cyclone collects some of the finer aerosols which then impact on the walls and are washed off into the collection reservoir. The tangential flow characteristics of the particles impacting on the inner walls of the cyclone result in lower shear stresses and a corresponding higher bioefficiency when compared to liquid impingers. Cyclones are also more conducive to high-volume sampling, because they operate with lower pressure drop, and hence require lower power. As well as being used as samplers themselves, cyclones are also frequently utilized as pre-separators in conjunction with other

sampling systems, as they are simple, inexpensive, and can effectively separate particles above a given size. Crook[9] concluded that of all inertial samplers, cyclones are probably the most appropriate for collection of dilute aerosols due to their large throughput capability, and because the liquid can be recycled to further concentrate the collected particles.

Electrostatic precipitators are devices that use electrical rather than inertial forces to collect aerosol particles. Typical electrostatic precipitators (ESPs) collect particles by two separate operations. First, a vacuum source draws in the air, which then passes by a corona discharge, or a lower voltage charging field, where the particles acquire an electrical charge. Second, the particles are attracted to a surface of opposite charge and collected. A thin liquid film is frequently used to wash the particles from the collection surface, and is recycled to concentrate dilute samples. Decker,[11] for instance, reported that organisms collected from 10,000 liters of air could be concentrated into 10 milliliters of collection liquid. The physical collection efficiency of non-inertial samplers, such as electrostatic precipitators, is not as affected by a decrease in particle size as are the inertial devices. In addition, since the electrical force is exerted directly on the particles and not on the whole volume of air, relatively little power is required to move large volumes of air through the sampler. Inertial samplers, on the other hand, use most of the power to drive

the air through the collector, and higher collection efficiencies are associated with exponential increases in power requirements. A comparison was made between a large volume electrostatic precipitator and two inertial devices (an all-glass impinger and an Anderson impactor); results showed the ESP sampler to be the only one capable of recovering quantities of airborne rabies virus.[12] ESPs have also been used to successfully collect airborne human respiratory disease viruses.[13] One potential disadvantage of ESPs is the production of nitrous oxides and ozone from the corona discharge, or the effect of a strong electric field for lower voltage operation, which may affect the viability of some microorganisms.

Thermal precipitators work by introducing a high thermal gradient across a narrow channel, through which the sample is passed. Airborne particles entering the channel will move in the direction of decreasing temperature by thermophoretic motion. If a sufficient gradient is applied, this type of sampler is reportedly very efficient at collecting small particles, i.e., 5 μm to less than 0.01 μm.[14] Similar to ESPs, air flows freely through the device; hence pressure drop is low. Collection rate is relatively low, however, and the high temperatures required to get good collection efficiency can affect the viability of microorganisms. Consequently, thermal

precipitators have been used primarily as a research tool, and have little application for bioaerosol collection.[15]

From a simple examination of the physical collection mechanisms involved in aerosol collection, most types of samplers can be eliminated based on their inability to satisfy the criteria set forth for a miniature, low-power, unattended bioaerosol sampler. The constraint for low cost and low power eliminates devices that require relatively large power due to substantial pressure drop, such as filtration units and most types of inertial devices. The requirement for collection into a liquid for detection with the new generation of analytical methods eliminates samplers that collect on a solid or semi-solid surface, such as agar plates. Maintaining the bioefficiency requires a relatively gentle collection mechanism, which must also be balanced with the desire to sample large volumes. Based on these considerations, the two samplers that most nearly satisfy the criteria are the cyclone and the electrostatic precipitator.

1.4 Sampler Evaluation

To determine the physical and bioefficiency of a sampler for a given microorganism, valid test procedures must be used. Henningson and Ahlberg[5] reviewed methods and procedures used in the evaluation of

samplers, primarily showing the lack of consistency and the varied conditions used in past sampler studies. Two types of test systems are possible: natural environments and controlled laboratory systems. Natural environments are typically complex, and data acquired under varying sampling conditions may be difficult to analyze. Complete sampler analysis should include testing under conditions closest to the proposed application, however. Under controlled laboratory conditions, the most important aspect of efficiency testing of samplers is the analysis of the collected aerosol. Both viable and total cell counts must be determined, and several microorganisms have been proposed as standards for test aerosols in the assessment of sampler bioefficiency.[4] These commonly used standards are *B. subtilis*, *S. marcescens*, and *E. coli*. These are traditionally used because they are relatively stable in aerosol form, they are readily available, and they are easy to culture. With few exceptions, the number of viable cells in bioaerosol sampling studies has been determined by cultivation,[5] though this method is relatively slow and not very precise.

Chapter 2. Literature Review

A review of the literature was made to investigate previous research into the fields of bioaerosol sampling, bioaerosol and general aerosol samplers (standard and miniature sizes), analytical detection techniques, miniature cyclones, and electrostatic precipitators. Henningson and Ahlberg[5] reviewed the literature on the evaluation of over 100 bioaerosol samplers from 1883 to 1993, and concluded that much work needs to be done to characterize the wide variety of samplers in current use. Henningson and Ahlberg's review, as well as one by Griffiths and DeCosemo,[4] provided several hundred references covering all types of samplers, traditional sampling techniques, testing procedures, and analytical techniques. Although the number of samplers used to collect bioaerosols is very large, "roughly equal to the number of investigators", Wolfe[16] concluded in 1961, very few have been tested thoroughly. In addition, several reviewers discussed the lack of thorough sampler evaluations, and stressed the urgent need for standard methods and test procedures for the development of bioaerosol sampling.[4,5,17] Many of the existing samplers have been developed for specific applications and would be unsuitable under alternate situations. In addition, many of the samplers that are in use today have received limited

evaluation with the knowledge of aerosol physics.[5] This is particularly so for small samplers, which have had very little characterization and development. A major reason for this, as stated previously, is the relatively recent advancements in detection sensitivity, which place different requirements on the front-end sampler, and now provide the opportunity for the miniaturization of samplers. Henningson and Ahlberg's review covered 89 studies on 67 different inertial devices, 14 studies on 6 different filtration samplers, and 6 studies on 7 different samplers using a mixture of other methods. This distribution indicates the relative past usage of each type of sampler used in bioaerosol collection.

2.1 Sampler Selection

A. Cyclone

Of the two samplers that most nearly meet the criteria set forth previously, the cyclone is the simpler collection device. Figure 1 is a schematic diagram of a typical cyclone. Separation of the particles is due to the centrifugal force caused by the swirling gas stream, which throws particles outward toward the cyclone wall. Opposing this motion is the inward drag force caused by turbulent gas flow toward the axis of the cyclone. All efficiency theories set up a balance between these two forces.[18]

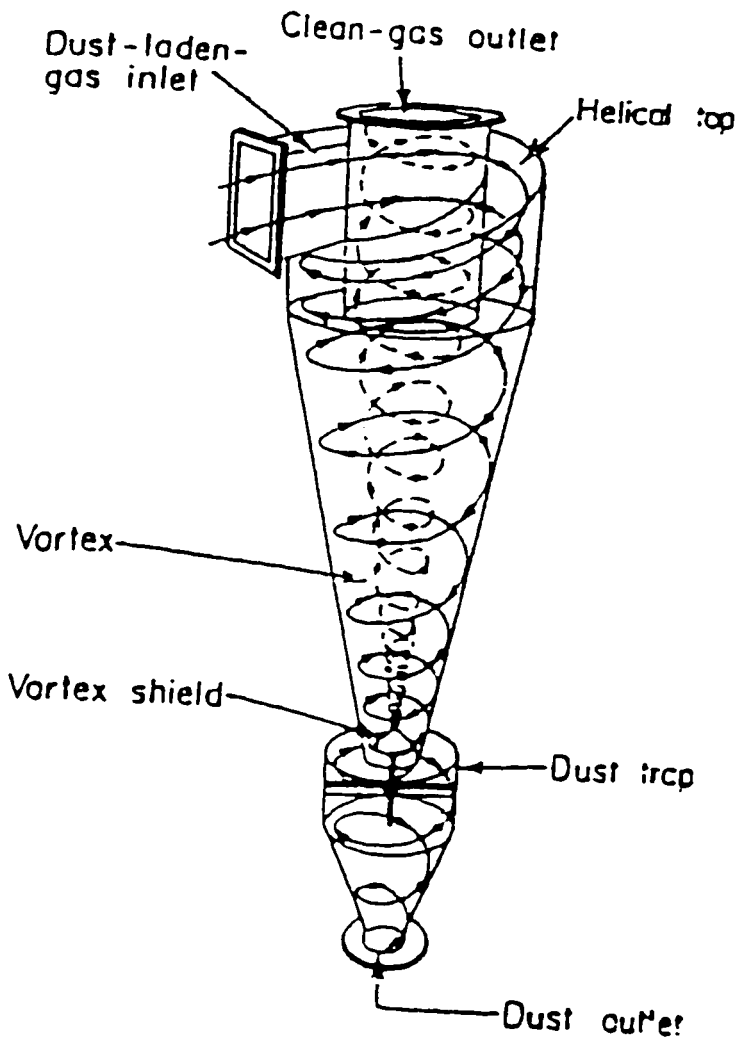

Figure 1. Schematic of a typical cyclone.[2]

Cyclone theory is complex, and many theoretical, semi-empirical, and empirical models have been developed with varying degrees of success.[3] Application of these models to a miniature device involves a large degree of uncertainty due to the empirical nature and complexity of cyclone design. Most models are limited to small ranges of geometric and dynamic similarities. Physical collection efficiency is strongly dependent on the sampling velocity and cyclone geometry. Increasing the sampling velocity will increase the physical efficiency, but higher shear forces are generated which would likely decrease the bioefficiency of collection. In addition, an increase in required sampling velocity requires greater power, and hence a larger vacuum source. Due to the empirical nature and complexity of cyclone design, however, the actual degree of loss in bioefficiency in relation to the physical efficiency for 1- 5 μm particle collection would have to be determined experimentally. A balance between the physical and bioefficiencies would need to be made by adjusting the sampling flow rate, and possibly the cyclone geometry. Because the collection mechanism is inertial, a miniature cyclone may not be able to collect particles less than 5 μm efficiently without requiring excessive flow rates, and hence may not be as conducive to miniaturization as the ESP. Several studies[18,19,20] show this efficiency dropoff with decreasing particle size, as well as the decreasing size of the cyclone

itself. Kim and Lee, hypothesized that reducing the cyclone body size reduces the residence time of the particles, and hence the collection efficiency. [19] Figure 2 shows typical efficiency curves generated for small cyclones as reported by Kim and Lee. The rapid drop in efficiency below 5 μm is clear from the figure. Other researchers have reported similar efficiency trends.[3,18]

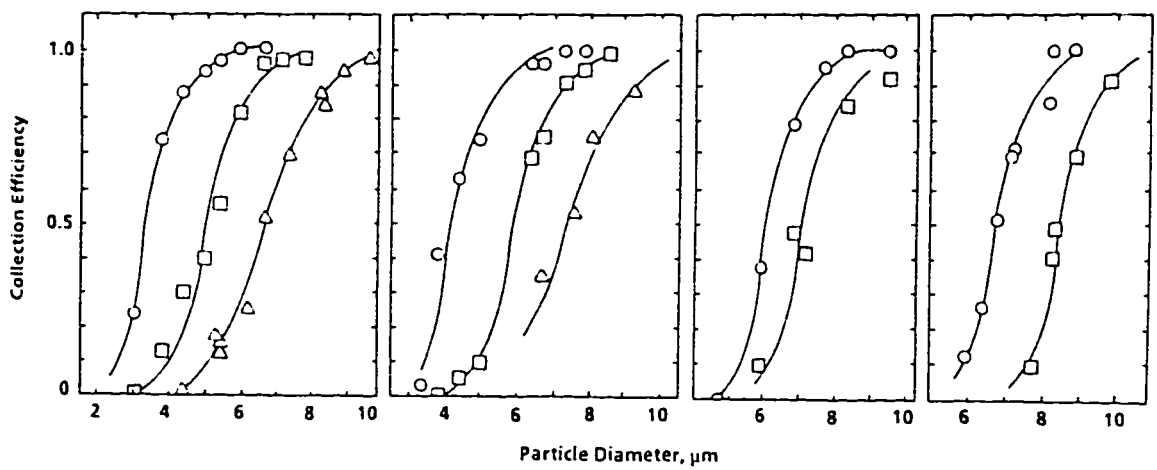

Figure 2. Measured collection efficiencies of several miniature cyclones (O = 18.4 lpm; □ = 12.4 lpm; Δ = 8.8 lpm).[19]

One model, the 10-mm cyclone, does show potential for improved collection efficiency at lower particle sizes and low to moderate flow rates, however, as shown by Chan and Lippmann and others.[21] An empirical correlation was developed by Chan and Lippmann as a function of collection efficiency, particle size, and flow rate. Figure 3 shows a plot of empirical and theoretical data for the cyclone, indicating its percent retention (physical efficiency) for particles from 5 μm to sub-micron sizes. Dirgo and Leith[18] reported relatively high physical efficiencies with the same cyclone for 1-5 μm particles, though the sampling flow rate was higher in their experiments.

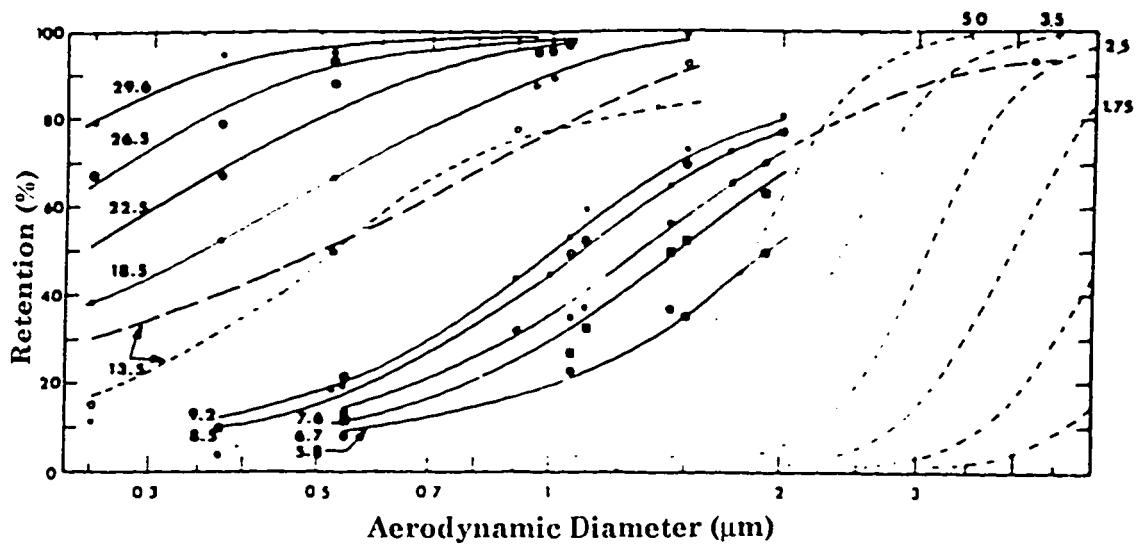

Figure 3. Collection efficiency of a 10-mm cyclone (Solid and dashed line curves computed by empirical theory; flow rates are in lpm).[21]

This device, the 10-mm cyclone, appears to have the potential to meet all of the criteria set forth for a miniature sampling system, provided the physical and bioefficiencies are acceptable.

B. Electrostatic Precipitator

Electrostatic precipitators have long been used to remove particulates from air, but, as reported by Burge and Solomon,[6] have not been routinely used in bioaerosol collection. As discussed previously, however, the ESP has the potential to meet our criteria as a miniature sampler. Decker[11] developed a large-volume ESP capable of concentrating 10,000 liters of air into 10 ml of collection liquid, with a physical collection efficiency for *B. subtilis* and *S. marcescens* in the range of 80-90%. Because the ESP separates particles from the air stream by electrical rather than inertial forces, the air handling power requirements are low, and hence can be scaled down effectively. There are two mechanisms for charging particles in an ESP: negative corona charging, and field charging.[22] For the corona mechanism, with voltages up to 100,000 V, gas molecules are ionized, which then flow towards the grounded plate. These molecules strike electronegative gases, thereby creating negative ions. This method is more effective for particles smaller than about 0.2 μm. Field charging occurs as negative ions are driven by the electric field onto the larger particles that intercept the field lines. Field

charging is more effective for particles larger than 1 μm,[22] which are primarily the particles of interest in respirable aerosol sampling. ESPs have a wide range of collection capabilities, extending well into the sub-micron particles. Masuda and Hosokawa[23] report 99-99.9% efficiency for 0.3 μm particles or smaller. This high efficiency is largely due to the electrostatic collection mechanism. The electrostatic force per unit mass on a particle can be as high as 3000 times the force of gravity for a 1 μm particle.[22] Winkler[12] showed that an ESP can be effective in collecting airborne rabies virus, and other researchers[12,13] have shown effective collection of airborne human respiratory disease viruses, airborne bacterial cells, and bacteriophages. These advantages are made at the expense of more complex design and construction considerations. Figure 4 shows a schematic of an ESP.

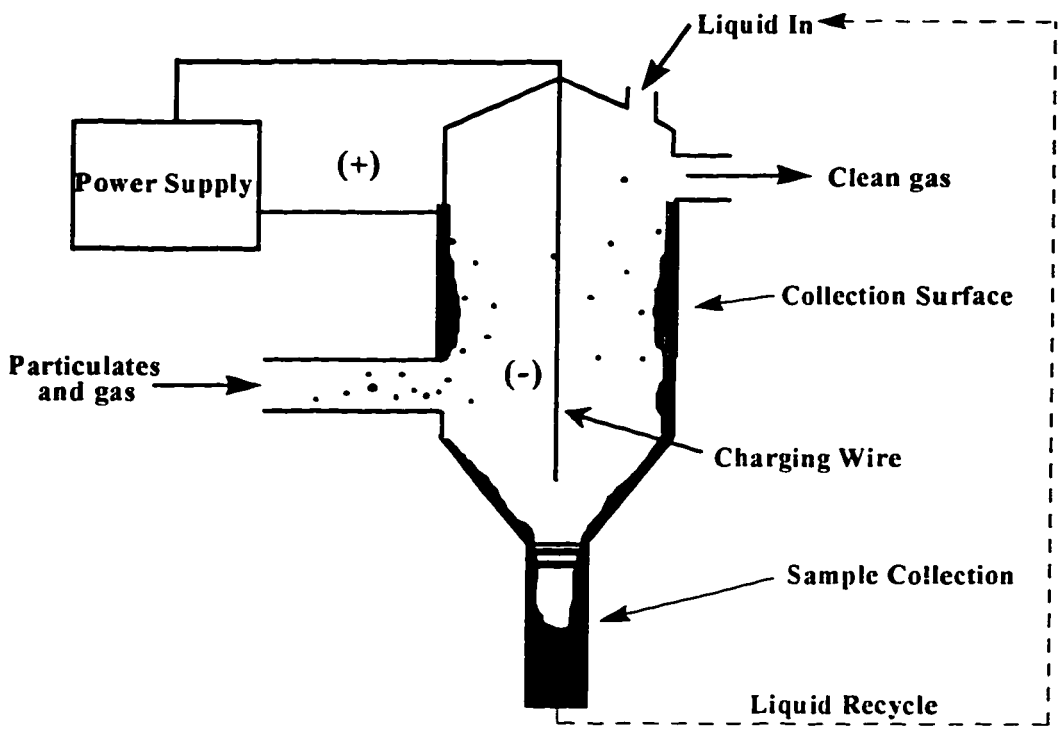

Figure 4. Schematic of an electrostatic precipitator.

Utilizing the cyclone correlation from Chan and Lippmann[21] for the 10-mm cyclone, and one developed by Masuda and Hosokawa[23] for an ESP, a comparison can be made between these two types of samplers to give a preliminary indication of the different power requirements for the cyclone and the ESP, and hence their ability to be scaled down. Assuming a collection of 10,000 particles 1 μm in diameter is desired in an atmosphere of 1,000 particles per liter of air, and that we want a 90% collection efficiency of these 1 μm particles. From Chan and Lippmann's equation (See Appendix B), using the given parameters for the 10-mm cyclone, a required volumetric flow rate of 18.5 liters per minute is calculated, which would require sampling 11.1 liters of air at a total sampling time of 36 seconds. A comparison can be made with a comparably sized ESP, in which the inner collection surface area of the cyclone is assumed to be the same size as the collection surface of the ESP. Using the correlation of Masuda and Hosokawa for the ESP gives a required flow rate of 4.4 liters per minute, at a total collection time of 2.5 minutes. Clearly, the sampling time is longer for the ESP, but the required flow rate is much lower; hence power requirements are less. Moreover, the cyclone sampling flow rate could not be reduced to lower the power requirements and retain the same efficiency. The ESP, on the other hand, has the additional applied electric field that may be

increased to improve collection efficiency without increasing the air handling requirements. Appendix B tabulates the results of the comparison, as well as the correlations and the assumed parameters.

Chapter 3. Hypothesis

The physical collection efficiency of two different microorganisms, *B. subtilis* and *S. marcescens*, will increase with increasing sampling flow rate in the cyclone and the electrostatic precipitator, providing that the particle size remains constant. The electrostatic precipitator will achieve higher levels of physical efficiency than the cyclone at low flow rates. In addition, the bioefficiency of the cyclone will decrease with increasing flow rate, while the bioefficiency in the electrostatic precipitator will remain relatively constant.

Chapter 4. Materials and Methods

Evaluation of the physical and bioefficiencies of a miniature cyclone and a miniature electrostatic precipitator was performed by aerosolizing suspensions of *B. subtilis* and *S. marcescens*, collecting the bioaerosols in the samplers, and performing a material balance to determine the desired efficiencies. The following sections outline the materials and methods used for these experiments.

4.1 Equipment

The miniature ESP sampler used in this study was designed and constructed at SRI International. The design was similar to that shown in Figure 4. The ESP collection area was specified to be the same as the 10-mm cyclone, which has an interior collection area of 15.27 cm^2. The charging field for the ESP was generated by a 200 V power supply (Life Technologies, Gibco BRL Electrophoresis Power Supply, Model 250). The variation in the physical and bioefficiency with voltage was not determined in this study. The voltage selected was chosen empirically to give comparable collection efficiency to that of the 10-mm cyclone at the minimum voltage necessary. For the ESP to be acceptable in a miniature detection system, it is desirable

to have the power supply as small as possible. A preliminary estimate of the collection efficiency was made to determine amount of collection under this 200 V charging field prior to the actual tests, following the same procedure as outlined in the following sections, to verify its acceptability. Several preliminary runs were performed under varying flow rates to make this evaluation. The voltage for all experiments was 196 ± 1 V, and the current was 2 ± 0.5 mA. This gave a constant power of 0.39 W for all ESP trials.

The cyclone used in this study is commercially available, and was purchased from Dorr-Oliver (Doxie Type-A Cyclone). It is the same type as the 10-mm cyclones reported in the literature[18,21].

The apparatus used to generate and collect the bioaerosols is shown in Figure 5. It consisted of a disposable nebulizer (Hudson RCI, #1730 Up-Draft II Neb-U-Mist), calibrated vacuum gauges (Wika, 0-30"), a digital micro-manometer (Alnor, Model 530 Eco Series Manometer), a make-up air line with a humidifier (Hoescht, Liqui-Cel 5pcm-104), a compressed air line, a vacuum line controlled by a critical flow orifice, a mass flow meter (Sierra Mass Flow Meter, Sierra Instruments, Model 82152-20-2), and the cyclone or ESP sampler. This closed sampling system provided reproducible test conditions, and has been used previously at SRI International to perform physical and bioefficiency tests of a custom miniature cyclone with proteins.[24]

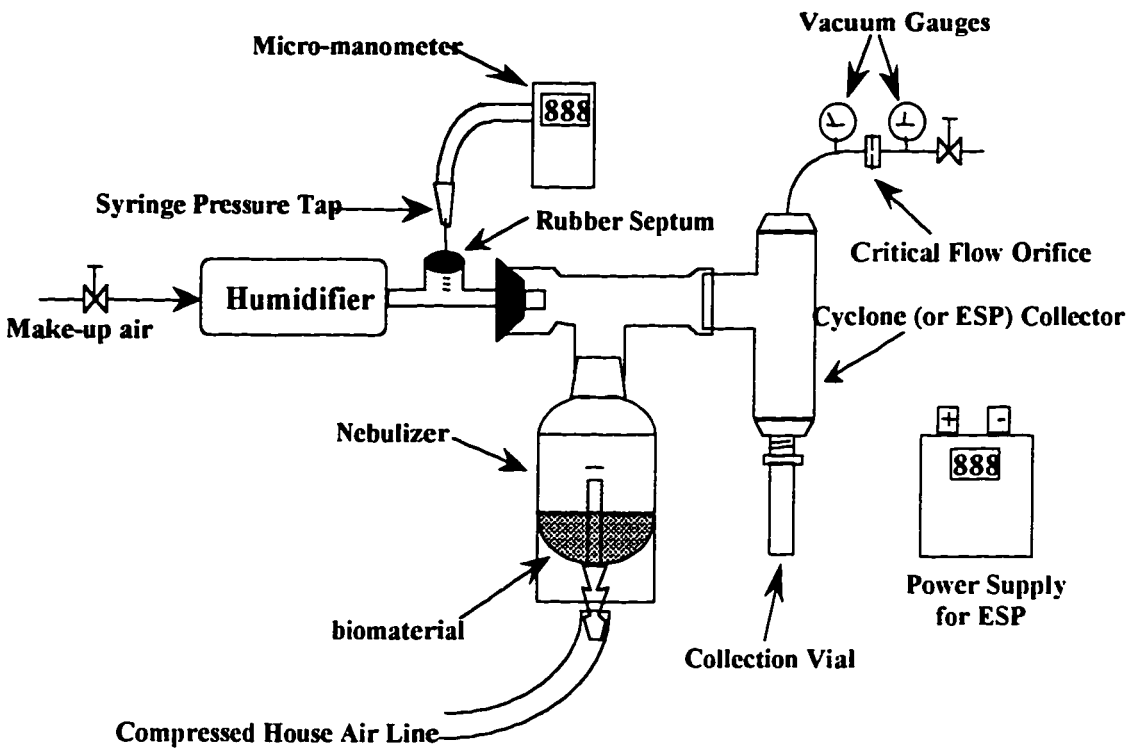

Figure 5. Apparatus for bioaerosol generation and collection.

4.2 Microorganisms

Serratia marcescens (SM) (ATCC #13880) was obtained as a freeze-dried culture from American Type Culture Collection (ATTC) in Rockville, MD. Upon receipt of *S. marcescens*, the freeze-dried culture was processed following ATTC's recommendations by re-hydrating the culture in 5 ml of Trypticase Soy Broth (TSB) and by streaking a loopful of the re-hydrated culture on a Trypticase Soy Agar (TSA) plate for individual colonies. After overnight incubation at 35 °C one single colony was picked and re-streaked on a TSA plate for purification. This plate was kept in the refrigerator and served as the master plate from which an inoculum was used to start an overnight culture in 5 ml TSB the day before the planned experiment. The culture was incubated at 35 °C. The bacterial suspension for each experiment (cyclone and ESP) was then prepared by diluting the overnight culture of SM in 50 ml of the sterile saline:ONP solution with 0.1 ml, a volume expected to give a final cell density of about $5x10^6$ CFU/ml.

Bacillus subtilis (BS) spores were obtained from a spore suspension provided by the US Army for SRI in 1991. The spore suspension had been stored in the dark in the refrigerator, and had a viability of about $3x10^8$ colony forming units/ml (CFU/ml). The spore suspension was diluted by transferring 6.5 ml to 54 ml of sterile saline:ONP. To remove large particles

and debris, the diluted stock suspension was centrifuged at 7000 RPM for 15 minutes. Since the spores measure between 1 μm and 3 μm in diameter, they should remain in the supernatant at this centrifugal force. After centrifugation the supernatant was clear but had a yellowish color, most likely due to the nutrients that were present in the stock spore suspension. The pellet obtained after centrifugation at 7000 RPM was substantial and most likely contained debris and clumps of deteriorated spores that had accumulated. This procedure proved to be adequate for the research, as sufficient spores were recovered (about $5x10^6$ CFU/ml).

The diluents for the overnight cultures of the test organisms consisted of sterile physiological saline (13 g/1500 ml water) and o-nitrophenol (ONP) at a final concentration of 0.125 mM. The ONP was added to the microorganism suspension to be able to measure concentration differences in the experiments, as described in the next section. The solution was prepared by adding 160 ml of a 0.2mM ONP solution to 640 ml of physiological saline. The 800 ml final volume of saline:ONP was sufficient for performing the experiments of this study. The saline:ONP solution was autoclaved for 30 minutes.

4.3 Determination of Physical Efficiency

The equation used to determine the physical efficiency (PE) is as follows:

$$PE(\%) = \frac{V_{tc}}{V_{fs}} \times 100$$

where V_{tc} is the total volume collected in the cyclone or ESP, and V_{fs} is the total volume fed to the sampler.

The total volume collected in the sampler, V_{tc}, was determined from two values: (1) the weight of the collection vial before and after each run, which gives the volume collected in the vial, and (2) the volume remaining on the walls of the cyclone or ESP. Direct weight measurements were made before and after each run using a Mettler AT250 balance (± 20 μg). The volume remaining in the cyclone or ESP after the runs was determined by rinsing the walls with a 0.2 mM tracer solution of ONP. The absorbance of the solution was then measured using a Hewlett Packard Diode Array Spectrophotometer (Model 8452A). This absorbance value was translated to concentration, and hence volume, by using a standard curve. The ONP standard curve generated for these experiments is in Appendix E-1.

The total volume fed to the sampler, V_{fs}, was determined from the following equation:

$$V_{fs} = V_{ni} - V_{nf} - V_{tf} - V_{ev}$$

where V_{ni} is the initial volume in the nebulizer, V_{nf} is the final volume in the nebulizer, V_{tf} is the volume remaining in the tee, and V_{ev} is the volume lost in the nebulizer by evaporation.

The initial volume in the nebulizer, V_{ni}, was 4.0 ml for each run, and was delivered by pippette. The final volume in the nebulizer, V_{nf}, was determined by direct weight measurements of the nebulizer with the liquid suspension before and after each run. A density for the both microorganism suspensions was determined by weighing a known volume of each solution, to convert the weight values to volume. The volume remaining in the tee, V_{tf}, was determined by weighing the tee before and after each run. It was also necessary to use a pre-weighed tissue to collect some of the liquid as the pieces were taken apart, because the liquid tended to collect at the junctions of the tee, and would otherwise spill. Finally, the volume lost in the nebulizer by evaporation, V_{ev}, was determined from an absorbance measurement of the remaining suspension in the nebulizer after each run. As discussed in the previous section, ONP was added to the stock microorganism suspensions to yield a final concentration of 0.125 mM. An initial absorbance measurement of this suspension was then compared to the

final absorbance measurement after the run, which was translated to a volume of liquid by the standard curve.

The system flow rate for sampling was set by first adjusting the nebulizer pressure to 15 psig, and then the vacuum until the desired flow rate, 5, 15, or 25 lpm, was obtained. The make-up air rate was adjusted to balance the system. Flow rates were set by means of a critical flow orifice in the vacuum line, and verified with the Sierra mass flow meter. A maximum sampling flow rate of 25 lpm was used as the upper limit, above which the required vacuum pump begins to be too large for use in a miniature sampling system. The nebulizer air and make-up air temperatures and relative humidities were measured at the beginning and end of each test session using an Omega Digital Thermo-Hygrometer (Model #RH411). The make-up air after humidification measured approximately 75% relative humidity at a temperature of 73 °F throughout the experiments, while the compressed air in the nebulizer measured approximately 20% relative humidity at 72 °F. Neither air lines were tested directly for pre-existing microorganisms, but test results during viability measurements of the collected samples showed that no other microorganisms were present besides the target microorganisms, based on the visual colony growths on the TSA plates. Moreover, any contaminants would have been immediately diluted and

plated on solid agar, and hence would not have the opportunity to grow, and therefore to reach a cell density that would have interefered with the viable cell counts of the target organisms.

The liquid suspensions were nebulized until a sufficient amount of liquid was collected in the collection vial for viability and total cell counts. Typical volumes collected ranged from 0.1 – 1.5 ml, with typical nebulization times ranging from 10 to 15 minutes.

The pressure drop through the cyclone and ESP samplers at 5, 15, and 25 lpm was also measured with a digital micro-manometer. The estimated power requirement was then determined as the product of flow rate and pressure drop for the cyclone. The ESP had additional electrical power, which was constant in these experiments. The electrical power was determined from the product of the applied voltage and current, which was 0.39 watts. The electrical power was then added to the air handling power to estimate the overall power required for the ESP.

4.4 Determination of Bioefficiency

The volume collected in the cyclone or ESP collection vial for the determination of physical efficiency was also used to determine the bioefficiency. Two values were measured: total cell (or spore) counts and viable counts. The motivation for determining the total cell count before and

after each run was to determine a "transfer efficiency", or how efficient the cells or spores were actually transferred. The transfer efficiency provides a more reliable measure than the physical efficiency of the "representative" nature of the sample. The transfer efficiency is useful, for instance, when a decrease in bioefficiency is found, as it can confirm if the decrease was simply due to fewer cells being transferred during the collection process, or if the decrease is in fact due to sampling.

For viable counts 0.05 ml or 0.1 ml volumes were removed, and 20 μl were removed for cell counts. Serial 10-fold dilutions were made by transferring the 0.05 ml or 0.1 ml volumes aliquots to 0.45 ml or 0.90 ml of diluent, respectively, which consisted of sterile physiological saline. The first transfer was made by adding 0.1 ml of the sample from the collection unit. A total of 4 serial dilutions were made. Two drops of 0.01 ml of each dilution were then placed on TSA plates. When the drops had dried in the agar, the plates were incubated overnight at 35 °C. The following day, colonies were counted in the drop areas that contained non-overlapping colonies. The maximum number of non-overlapping colonies that could be counted was about 16. The total number of viable bacteria present in the collection unit was calculated as colony forming units/ml (CFU/ml) by using the average number of colonies in the two drop areas of a given dilution, multiplying that

number with the dilution factor, and adjusting for the volume delivered, as the following example shows:

Counts: 6 and 8 at dilution 10^{-4}.

Calculated number CFU/ml: $7x10^{4}$ (dilution factor)$x10^{2}$ (plating of 0.01 ml in the drop area = $7x10^{6}$CFU/ml.

The percent bioefficiency was calculated by using the control value (non-treated sample) as the reference point. For example if the control value was 6.0×10^{6} CFU/ml and the CFU/ml of a treated sample was 3.0×10^{6}, the bioefficiency is 50%.

A hemacytometer was used to count particles (bacterial cells or spores) with a microscope. The layout of a hemacytometer has five large squares on each side, and holds a volume of 1 µl. Each side of the hemacytometer was filled with the tip of a pipetter holding 10 µl of the sample. To obtain the particle count/ml the following formula is used: *Total number of particles* in 10 large squares $\times 10^{3}$ = total particles/ml.

For counting *Serratia marcescens* the eyepiece used was 40x, and for counting the *Bacillus subtilis* spores the eyepiece used was 100x.

Table 2 outlines the experiments that were performed for the determination of the physical and bioefficiency.

Table 2. Experiments for physical and bioefficiency measurements.

Run #	Sampler	Organism	Flow Rate (lpm)
1	Cyclone	*B. subtilis*	5
2	Cyclone	*B. subtilis*	15
3	Cyclone	*B. subtilis*	25
4	Cyclone	*S. marcescens*	5
5	Cyclone	*S. marcescens*	15
6	Cyclone	*S. marcescens*	25
7	ESP	*B. subtilis*	5
8	ESP	*B. subtilis*	15
9	ESP	*B. subtilis*	25
10	ESP	*S. marcescens*	5
11	ESP	*S. marcescens*	15
12	ESP	*S. marcescens*	25

[Note: each run was performed three times.]

4.5 Aerosol Size Distribution

The particle size distributions of both organisms at 5, 15, and 25 lpm were measured with a Malvern Particle Sizer (Malvern Instruments, Series 2600c Droplet and Particle Sizer), by nebulizing the suspensions and letting the resulting bioaerosol pass through the Malvern's laser beam. The data generated by the Malvern Particle Sizer was taken and put into a spreadsheet program that determines a weighted curve fit, and therefore a more accurate value for the mass median diameter (MMD) and geometric standard deviation (GSD). The details of this curve fitting routine are presented in Appendix C.

To correlate the particle size distribution data from the nebulizer to the collection performance of the cyclone and the ESP, it was necessary to transform the particle size data at a given flow rate to volumetric data, and then to back out an effective particle cut diameter, based on the collected efficiency at the same flow rate. This cut diameter was assumed to be the diameter at which everything below it was collected, and everything above it was not collected. A volume fraction plot was generated from the particle size data, from which a corresponding cumulative fraction less than a given diameter was determined using the experimentally determined collection efficiency. This cumulative fraction number was then used with particle size

distribution plots for both organisms to find the corresponding effective cut diameter for the given flow rate and sampler.

Table 3 summarizes the equipment and materials used for these experiments.

Table 3. Equipment and material summary.

Instrument/Material	Specifications
Pressure Measurements	Wika, 0-30" Vacuum gauges Alnor, Model 530 Eco Series Manometer
Weight Measurements	Mettler AT250 balance (+/- 20 μg)
Flow Measurements	Sierra Mass Flow Meter, Sierra Instruments, Model 82152-20-2
Absorbance Measurements	HP model 8452A Diode Array Spectrophotometer
ESP Power Supply	Life Technologies, Gibco BRL Electrophoresis Power Supply, Model 250
Nebulizer	Hudson RCI, #1730 Up-Draft II Neb-U-Mist
Humidifier	Hoescht, Liqui-Cel 5pcm-104
Humidity Measurements	Omega Digital Thermo-Hygrometer Model #RH411
Particle Size Measurements	Malvern Instruments, Series 2600c Droplet and Particle Sizer
Cyclone Sampler	Doxie Type A Cyclone, Dorr-Oliver Inc.
ESP Sampler	SRI International
Bacillus subtilus	ATCC #13880, American Type Culture Collection (ATTC) in Rockville, MD.
Serratia marcescens	Provided by the US Army for SRI Project 2913-8

Chapter 5. Experimental Results

The presentation of the experimental results of this study is divided into six sections. The first section presents the aerosol size distribution data of both microorganisms, at each of the tested flow rates used in the cyclone and ESP runs. The second and third sections present the physical efficiency results for the cyclone and the electrostatic precipitator, respectively. The fourth and fifth sections present the bioefficiency results for the cyclone and the electrostatic precipitator, respectively. Finally, the sixth section presents data on the power requirements of both samplers.

5.1 Aerosol Size Distribution Data

The particle size distribution data was obtained for both microorganisms at 5, 15, and 25 lpm, as the material came out of the nebulizer. Figure 6 presents the results of the particle size measurements and analysis, each value being determined from an average of 3 to 5 runs each. Figures 7 and 8 present the particle size distributions for *B. subtilis* and *S. marcescens*, respectively, at 5, 15, and 25 lpm. Appendix E presents a sample particle size distribution as generated from the Malvern Particle Sizer.

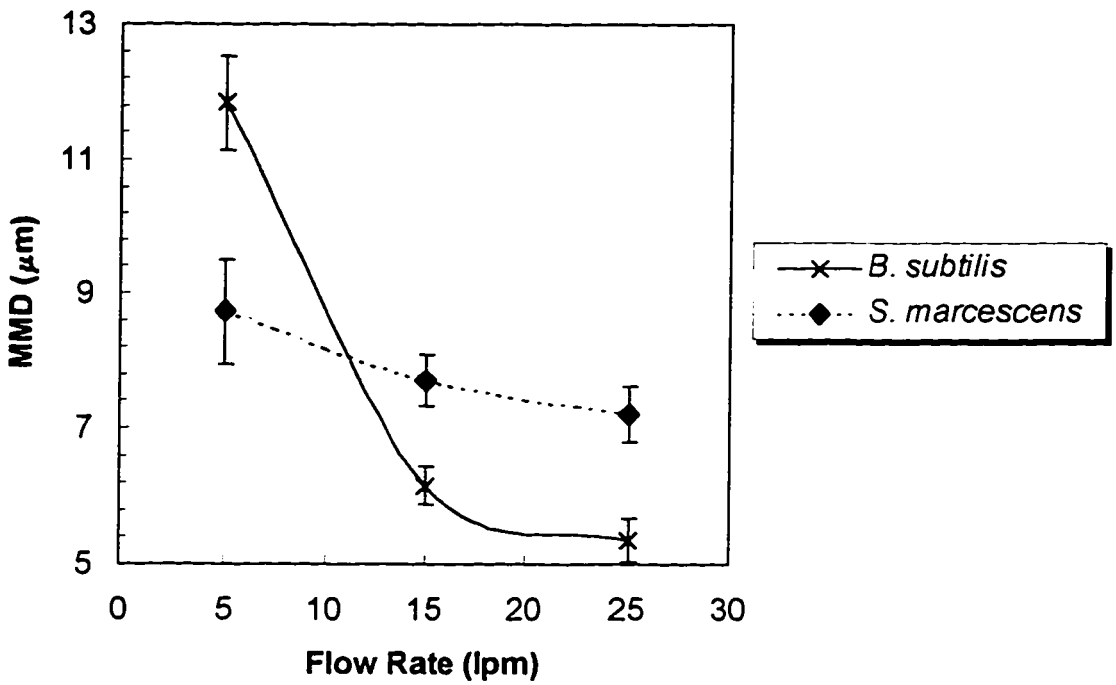

Figure 6. MMDs of *B. subtilis* and *S. marcescens*.

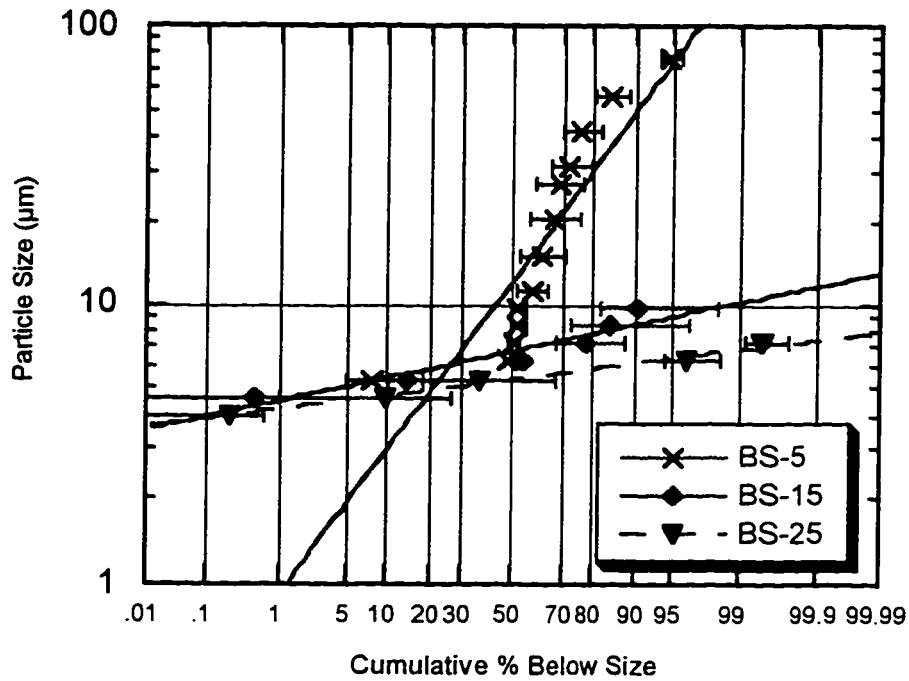

Figure 7. Particle size distributions of *B. subtilis*.

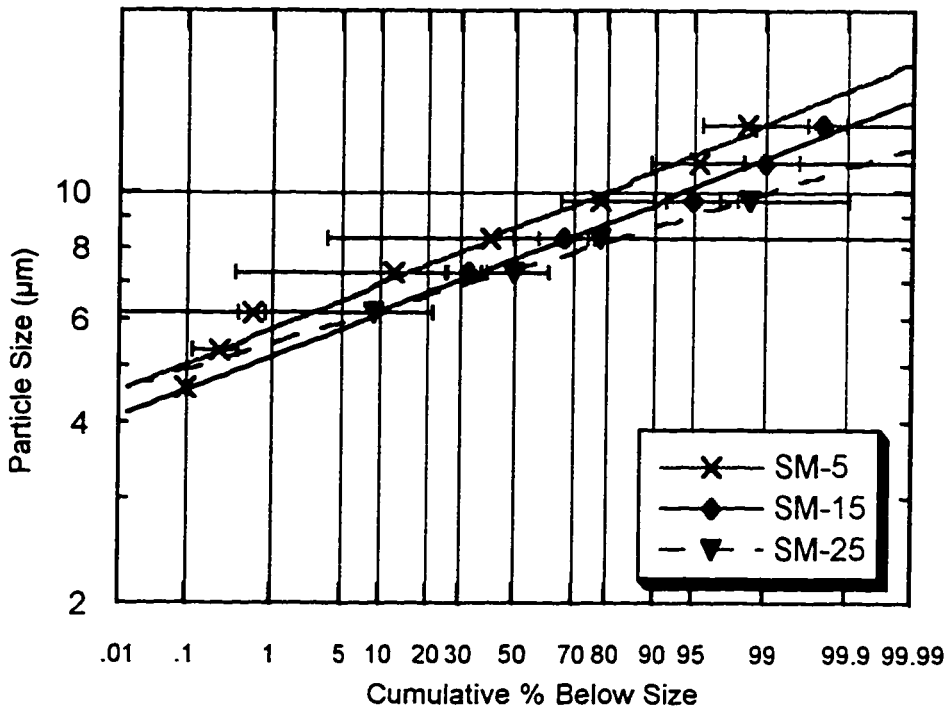

Figure 8. Particle size distributions of *S. marcescens*.

Since the particle size changed with the system flow rate and the collection efficiency of the cyclone and ESP also changed with system flow rate, it was necessary to correlate the particle size distribution data from the nebulizer to the collection performance of the cyclone and the ESP. Figure 9 shows a typical aerosol distribution plot generated from the particle size data. From this figure, the experimental collection efficiency was used to determine the corresponding cumulative fraction less than a given diameter. This cumulative fraction number is then used with Figures 7 and 8 to find the corresponding effective cut diameter for the given flow rate, sampler, and organism. The results of this analysis are presented in Figure 10, which shows how this effective cut diameter changes with sampler and flow rate.

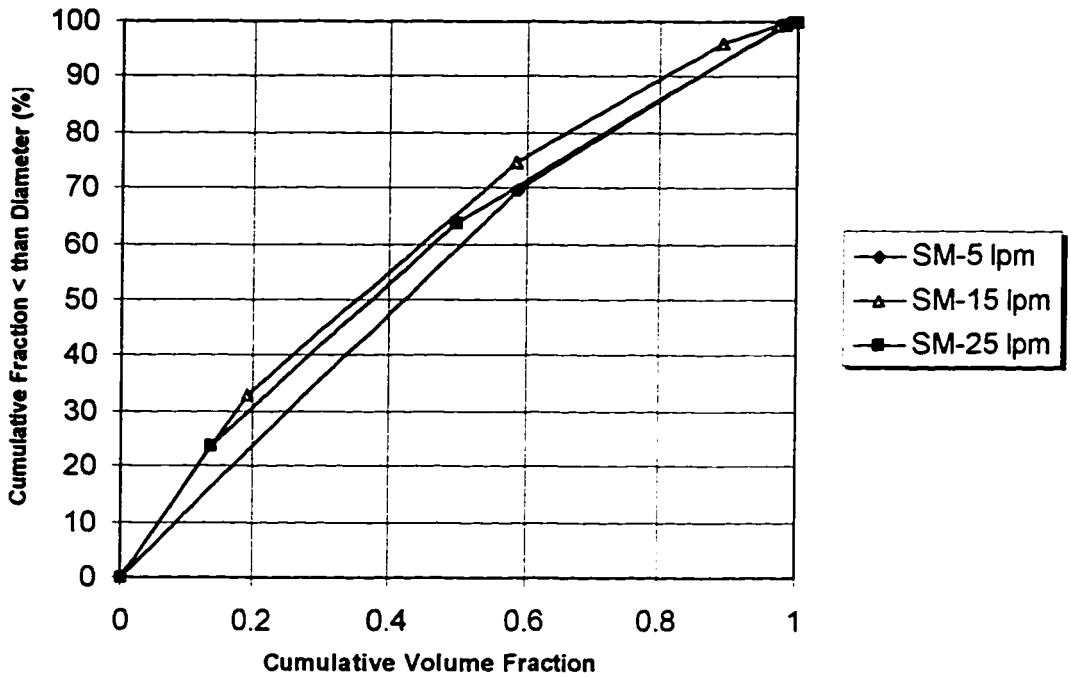

Figure 9. Plot to determine cumulative fractions for *S. marcescens*.

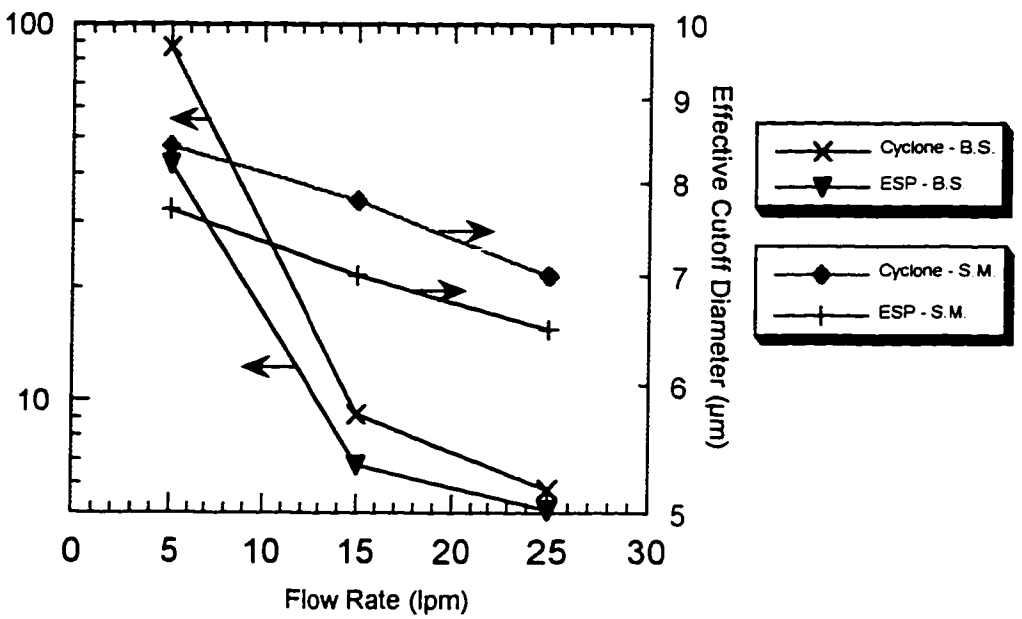

Figure 10. Effective cutoff diameters.

5.2 Cyclone Physical Efficiency Data

Physical efficiencies for each of three repetitions for the cyclone with *B. subtilis* averaged 43% ± 4% at 5 lpm, 32% ± 2% at 15 lpm, and 27% ± 6% at 25 lpm. For *S. marcescens*, the physical efficiencies averaged 51% ± 3% at 5 lpm, 37% ± 4% at 15 lpm, and 30% ± 6% at 25 lpm. ANOVA analysis showed that there is a difference in the measured physical efficiencies between the two organisms at each flow rate, at a 95% confidence level. The physical efficiency results of the cyclone collector are plotted as a function of flow rate in Figure 11 of the next section, along with the ESP results. Complete experimental data and material balance calculations are presented in Appendix D.

It is clear from Figure 11 that the physical efficiency of the cyclone decreased with increasing flow rate for both microorganisms. This observation is the opposite that is expected from theory, if the particle size is constant at all conditions. As was shown in section 5.1, however, the particle size did in fact decrease with increasing flow rate in the nebulizer system.

5.3 Electrostatic Precipitator Physical Efficiency Data

Physical efficiencies for the ESP with *B. subtilis* averaged 75% ± 5% at 5 lpm, 72% ± 7% at 15 lpm, and 69% ± 5% at 25 lpm. For *S. marcescens*, the

physical efficiencies averaged 69% ± 3% at 5 lpm, 71% ± 4% at 15 lpm, and 66% ± 5% at the 25 lpm flow rate. ANOVA analysis showed that there is not a difference in the measured physical efficiencies between the two organisms at each flow rate, at a 95% confidence level. The results for physical efficiency of the ESP are plotted in Figure 11, along with the physical efficiency results for the cyclone.

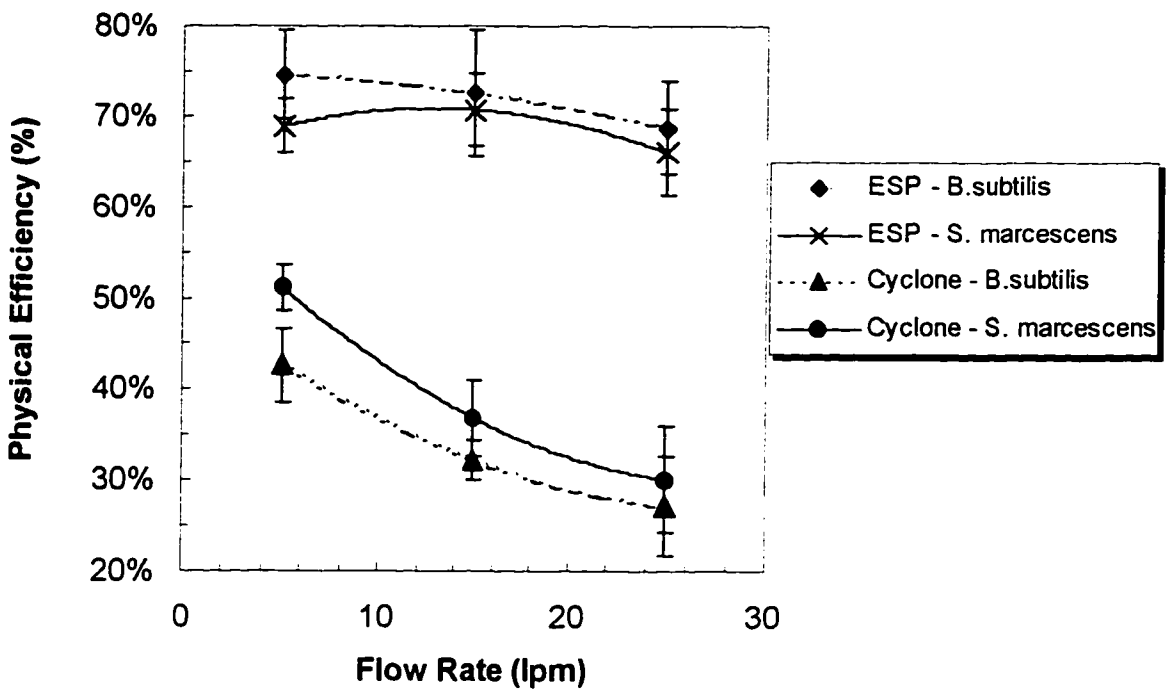

Figure 11. Cyclone and electrostatic precipitator physical efficiencies.

5.4 Cyclone Bioefficiency Data

Both the total cell concentrations and the viable cell concentrations were examined in determining the bioefficiency. For *S. marcescens* sampling with the cyclone, the total cell count in the control suspension sampled at the beginning of the experiment was about 3 times higher than the number of colonies observed on the plates: 1.6×10^7 particles/ml compared to 5.2×10^6 CFU/ml. The particle count in the samples obtained from the intermediate flow rate runs (15 lpm) was similar to that in the control sample and the bioefficiency was 100%. The slight decrease in bioefficiency in samples 1-C-S-15 and 3-C-S-15, 77% and 87% respectively, is not considered significant (See Discussion).

When sample 1-C-S-25 was examined microscopically it was noticed that the cell count was down to 72% of the control value. Another microscopic examination of the untreated control cell suspension also revealed a decrease in cell counts. There was some cell debris and what looked like some cell clumping in the sample. The cell count was also down in samples obtained from runs 2-C-S-25 and 3-C-S-25. Since the cell count was down in the untreated control sample, that count was used to calculate the percent of total cells recovered of the runs obtained at 25 lpm and 5 lpm.

When the plates used for viable counts were inspected the following day, the bioefficiency was 100% for the three samples.

The cell counts at 5 lpm were also down, with values between 49% and 88%. The average bioefficiency was down to 69%. A number of repeat experiments would need to be performed to determine how significant the decreases are, especially with one of the samples, namely 2-C-S-5, exhibiting a bioefficiency of 100%.

For *B. subtilis*, the total spore counts of the intermediate flow rate ranged between 64% and 100%. The bioefficiency of these samples was close to 100%. The total spore count was down to below detectable levels with the three samples obtained from the 25 lpm and 5 lpm runs. The bioefficiency was also down with between 5.5% and 33.7% for the samples obtained at 25 lpm, and between 1.4% and 5.5% for the samples obtained at 5 lpm. The average cyclone bioefficiency values as a function of flow rate are presented in Figure 12 of the next section, along with the ESP results.

5.5 Electrostatic Precipitator Bioefficiency Data

For *S. marcescens* sampling with the ESP, the number of cells present in the samples obtained after the three runs at 15 lpm, was equivalent to 100% with values similar to the control. The bioefficiency of these samples was also 100%. The total cell count for the samples obtained after the

highest and lowest flow rate runs was slightly down with an average of 71% at 25 lpm and 66% at 5 lpm. The bioefficiency of the samples at 25 lpm was between 56% and 94%, and between 78% and 100% for the samples obtained at 5 lpm.

As was observed in the experiments with the cyclone, the total cell count was down in the untreated control of the runs using 25 lpm and 5 lpm. A sample from the untreated cell suspension was therefore examined microscopically each time a treated sample was counted and the number of cells obtained was used to calculate the percent cells that were present in the collection unit. For *B. subtilis*, the percent spore count in the samples obtained from the intermediate flow rate runs (15 lpm) was between 76% and 100% of the control value. The bioefficiency of these samples was about 100%. The total spore count in the samples obtained from the 25 lpm runs was between 67% and 87%, with a bioefficiency between 58% and 100%. The total cell spore was between 27% and 44% for the samples obtained from the 5 lpm runs, with the bioefficiency down to between 13% and 72%.

ANOVA analysis showed that there was not a difference in the measured bioefficiencies and the transfer efficiencies, at a 95% confidence level. In other words, when the total cell or spore counts were down, there was a similar decrease in bioefficiency.

Figure 12 presents the average ESP bioefficiency results, along with the cyclone results.

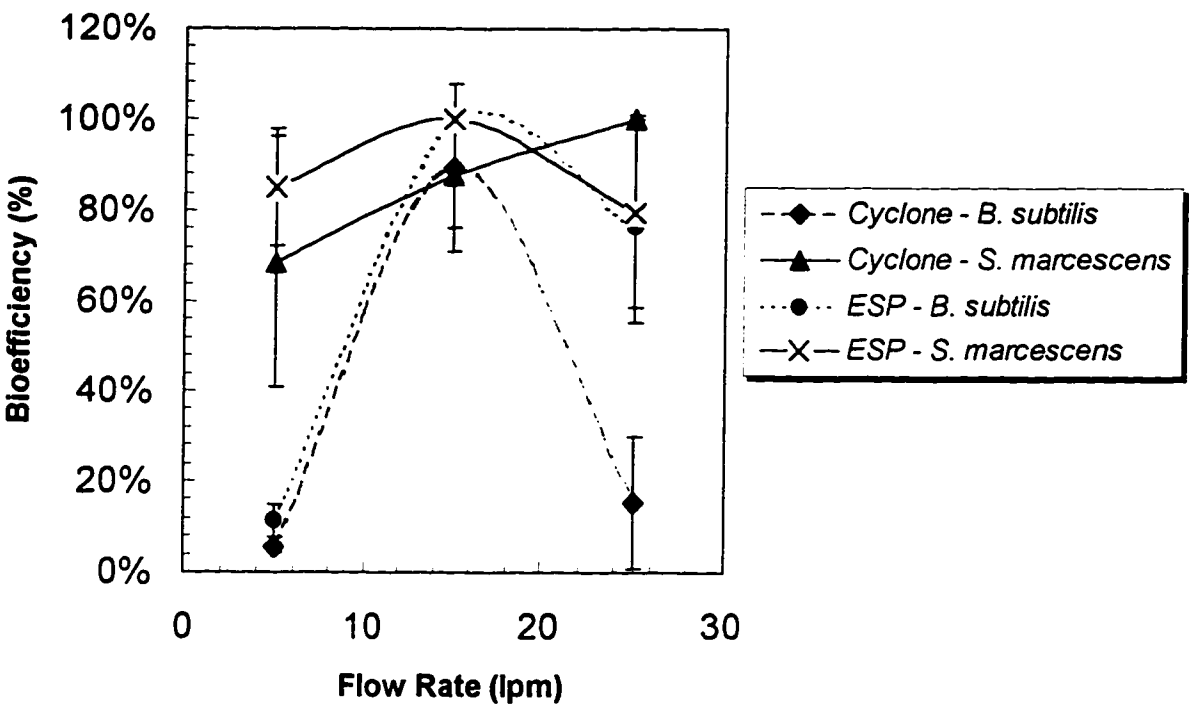

Figure 12. Cyclone and electrostatic precipitator bioefficiencies.

5.6 Power Requirement Data

As expected, the power requirements for the cyclone increased more rapidly than the ESP with increasing flow rate, as seen in Figure 13. At 5 lpm, the pressure drop is relatively low in both samplers, and the added electrical field makes the ESP require more power. The difference becomes more dramatic, however, at 15 and 25 lpm, as the cyclone air handling requirements increase much more rapidly than the ESPs. At 15 and 25 lpm, the power requirement for the cyclone was found to be 2.68 and 9.33 W, respectively. For the ESP at 15 and 25 lpm, the power requirement was found to be 0.89 and 2.26 W, respectively. Appendix D-5 contains the experimental data.

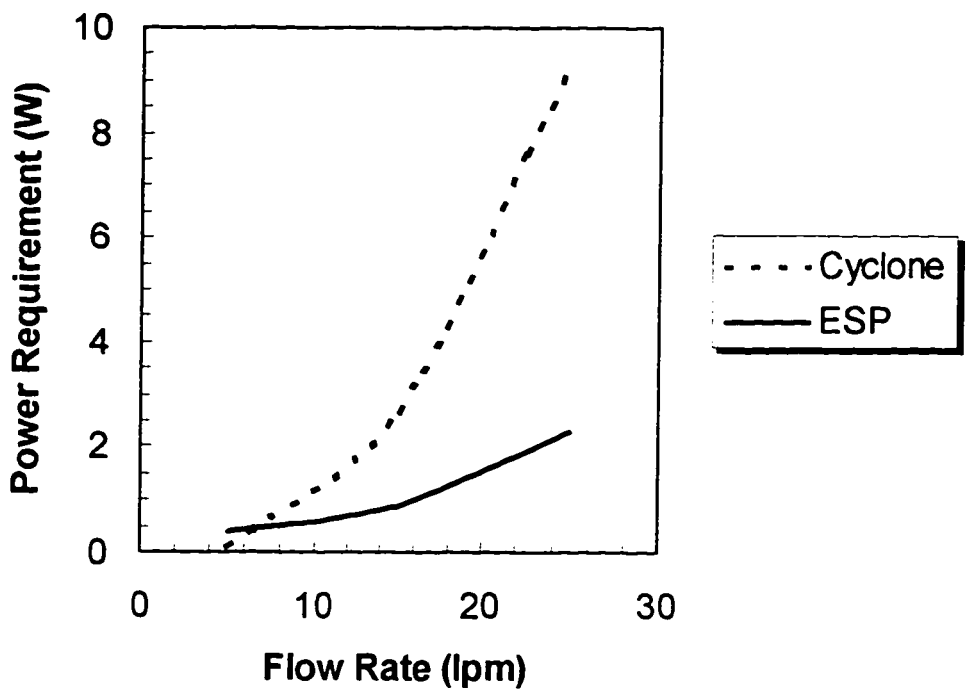

Figure 13. Comparison of power requirements for the cyclone and ESP.

Chapter 6. Discussion

1. Physical Efficiency.

As was seen in Figure 11, the physical efficiency of the cyclone decreased with increasing flow rate for both microorganisms. This is opposite the trend expected from theory, if the particle size remained constant. The aerosol size was found to decrease with increasing flow rate in the nebulizer system. Since the cyclone collects particles based on mass, decreasing the size of the particles (assuming constant density) will decrease the collection efficiency. This decrease in particle size is likely due to evaporation caused by the increase in flow rate of the make-up air, which had a measured RH of 75%. It was also observed that at the higher flow rates (15 and 25 lpm) liquid tended to collect in the tee section, hence increasing the opportunity for evaporation and reduction in droplet mass. At 5 lpm, however, very little liquid would remain in the tee portion, with the bulk of the sample either falling back into the nebulizer for re-nebulization, or being delivered to the cyclone. It is also possible that this decrease in particle size occurred in the tee section because of impaction of the droplets at the higher flow rates. The tee section reduced down to the cyclone inlet, which was roughly half the diameter of the tee. This abrupt change in diameter would cause a change in the streamlines, and particles or droplets

with sufficient mass would be impacted at the junction and collect there. Thus smaller particles would make it into the sampler at higher flow rates, which would again result in reducing the collection efficiency with increasing flow rate, as was seen experimentally.

It was noted that the collection efficiency for *B. subtilis* was consistently less than for *S. marcescens*. This was because the aerosol volume distribution of *B. subtilis* was smaller than *S. marcescens*, as shown in section 5.1. As individual particles, *B. subtilis* spores are approximately 1.5 μm in diameter, while *S. marcescens* is approximately 10 μm in length, and 2 μm in width. This difference in shape, spherical versus rod-shaped, may also be a major factor in the aerodynamic differences between the two in aerosolized form.

It was also found that the ESP exhibited a similar trend to that of the cyclone, that is, the decrease in physical collection efficiency with increasing flow rate, although this trend was not as strong as with the cyclone. The cyclone, which collects by an inertial mechanism, is much more influenced by a change in particle size than the ESP, which collects primarily by an electrostatic mechanism. The decrease in efficiency of the ESP with increasing flow rate may be due to the shortened residence time. This would be particularly evident at lower voltages, such as the operating voltage used

in this study. If this supposition were true, higher charging field strengths would be expected to decrease the necessary collection area and residence time required for collection, and improve the collection efficiency at the higher flow rates tested. The variation in the physical and bioefficiency with voltage was not determined in this study, but could produce significantly different results at higher voltages. It is likely that the physical efficiency would increase and the bioefficiency decrease with increasing voltage.

As discussed in section 5.2, the decrease in average particle size of the droplets with increasing flow rate explains the results obtained for the decrease in physical efficiency with increasing flow rate. It was also observed that the aerosol density decreased significantly with increasing flow rate. This may also explain the apparent increase in physical efficiency for the cyclone at 5 lpm, as the particles would have a greater tendency to agglomerate together and be collected at higher aerosol particle densities.

The material balance used in determining physical efficiency did not include liquid brought in by the make-up air. The air was measured to be at 75% relative humidity, however, so the probability for added mass to the system was small, but some additional mass may have entered in and thus artificially increased the physical efficiency by some amount. This value was

constant, however, and any difference would likely have been seen in each of the experiments, thus the trends found would not have been affected.

In conjunction with the efficiencies of the samplers, the power requirements determined at various flow rates also gives information on the suitability of each device as a miniature collector. As was shown in section 5.6, the cyclone power requirements increased much more rapidly than the ESP with increasing flow rate. At 15 lpm, for instance, the cyclone would require 2.68 W to operate, whereas the ESP would only require 0.89 W, thus decreasing the overall system size.

2. Bioefficiency.

For *S. marcescens* the transfer efficiency with both the cyclone and the ESP at the intermediate flow rate was 100%. The 94% transfer efficiency seen with the cyclone sample 3-C-S-15 is statistically within the error of the measurement, particularly considering the small volume (1μl) that was used for counting the cells and the fact that only three runs were performed. To obtain more reliable values and determine the error range more accurately, more data points would be required.

The bioefficiency in both the cyclone and ESP generated samples correlated well with the transfer efficiency. The small decrease in

bioefficiency with samples 1-C-S-15 and 3-S-C-15 is considered insignificant, and can be attributed to small variations in the volume during the dilution and plating process.

The average transfer efficiency of *S. marcescens* in both the cyclone and ESP samples generated with the highest and lowest flow rate appears to have decreased significantly from the control value. It was shown by ANOVA analysis that there was a positive correlation between the bioefficiency and the transfer efficiency at a 95% confidence level. In other words, if the bioefficiency was low, the transfer efficiency was also low by roughly the same amount. This indicated that the decrease in bioefficiency was not due to the sampling process, but to fewer viable cells or spores being transferred in the nebulization and collection process.

For the *B. subtilis* spores the transfer efficiency was also the highest at the intermediate flow rate. When the lowest and highest flow rates were used with the cyclone, the transfer efficiency could not be determined, as few if any spores were present in the field of view upon microscopic evaluation. The spore count was therefore below detection limits. The total spore count after treatment was consistently higher than the viable counts. This can be explained if the *S. marcescens* plating efficiency was less than 100%, which means that not all bacteria present in the sample were able to form visible

colonies on an agar plate. This is a wide spread phenomenon among microorganisms that are plated on a solid surface such as agar. The decrease in total cell counts in the untreated control observed in both the cyclone and ESP experiments at the beginning of the runs could be explained by a likely adverse effect on the bacteria maintained in the saline:ONP solution. In each case, the bacteria had been suspended in the diluent for about 2 hours. It is possible that a certain fraction of the bacteria may have been extremely sensitive to the ONP present at a final concentration of 0.025 mM. Some cell debris and clumps of cells were observed microscopically. The observation that the bioefficiency remained at about 100% can be explained by the fact that those bacteria sensitive to the ONP are those that would not have been able to form visible colonies on the plate.

Discrepancy between the total spore count and bioefficiency after treatment of the *B. subtilis* spores is most likely due to nonviable spores that remained in the supernatant after centrifugation which was a step used in the preparation of the spore sample (See Materials and Methods).

The small volume of samples collected (between 0.2 and 0.3 ml), required that the dilution process be scaled down. Instead of using the usual 1 ml of sample and 9 ml of diluent for the dilutions, 0.1 ml and in some cases 0.05 ml samples were used and 0.9 ml or 0.450 ml of diluent was used. Also,

volumes of 0.01 ml instead of the usual 0.1 ml were used to plate the organisms. The use of small volumes increases the margin of error. With a bacterial population of between 10^6 and 10^7, small variations in the volumes used during the diluting and plating process may extensively affect the margin of error.

It appears that the ESP is superior in collecting samples that have a higher total particle count and bioefficiency compared to the cyclone. This is especially the case when small particles such as *B. subtilis* spores are used. On average, the spores are about 1 -3 μm in diameter compared to the rod shaped *S. marcescens,* which measures about 10 μm in length and 2 μm in width. However, it is possible that size is not the only determinant for efficient transfer. Compared to vegetative bacteria, such as *S. marcescens*, spores are highly dehydrated and it could be that the degree of hydration may play a role in the efficient transfer of the nebulized particles.

Chapter 7. Conclusions

It was shown that both bacterial spores and vegetative bacteria can be nebulized and collected with either a cyclone or an ESP as collection devices. The physical efficiency of the ESP was consistently better than the cyclone, at all flow rates, and for both microorganisms. The ESP showed a 30% increase in physical efficiency on average. It also appears that the ESP is superior to the cyclone for both transfer efficiency and bioefficiency, with an average 10% increase over the cyclone. In addition, the power requirements for the ESP were found to be much lower than the cyclone as the sampling flow rate increased to 15 and 25 lpm.

Based on the overall results for both physical and bioefficiency, as well as the power requirements determined for each device, it would be recommended that the ESP be the selected sampler for further analysis, particularly to investigate the enhanced performance that would likely result at higher voltages. The ESP, therefore, appears to show greater potential than the cyclone to become the sampling device of choice for use in a miniature bioaerosol detection system.

References

1. "Bioaerosols in the Environment.", Cox, C.S. and C.M. Wathes, in *Bioaerosols Handbook*, Chapter 2 (1995).

2. "Gas-Solid Separations.", Perry, R., and D. Green, Perry's Chemical Engineers' Handbook, sec 20 (1984).

3. "Design and Performance of Miniature Cyclones for Respirable Aerosol Sampling.", Saltzman, B.E. and J.M. Hochstrasser, *Environ. Sci. Technol.*, Vol. 17, No. 7, pp. 418-424 (1983).

4. "The Assessment of Bioaerosols: a Critical Review.", Griffiths, W.D. and G. A. DeCosemo, *J. Aerosol Sci.*, Vol 25, No. 8, pp. 1425-1458 (1993).

5. "Evaluation of Microbiological Aerosol Samplers: a Review.", Henningson, E. W. and M. S. Ahlberg, *J. Aerosol Sci.*, Vol 25, No. 8, pp. 1459-1492 (1994).

6. "Sampling and Analysis of Biological Aerosols.", Burge, H. A. and W. R. Solomon, *J. Aerosol Sci.*, Vol 21, No. 2, pp. 451-456 (1986).

7. Hinds, W.C., *Aerosol Technology*, 2nd Edition, Wiley, New York (1982).

8. "Dust and Mist Collection.", Lunde, K. E. and C. E. Lapple, *Chem. Eng. Prog.*, Vol. 53, No. 8, pp. 385-391 (1957).

9. "Inertial Samplers: Biological Perspectives.", Crook, B., *Bioaerosols Handbook*, Chapter 9 (1995).

10. "A Cyclone Separator for Aerosol Sampling in the Field.", Errington, F. P. and E. O. Powell, *J. Hyg. (Camb.)*, 67: 387-399 (1969).

11. "Advances in Large Volume Air Sampling.", Decker, H. M., et al., *Contamination Cont.*, 8:13-20 (1969).

12. "Airborne Rabies Virus Isolation.", Winkler, L.U.G., *Bulletin Wildlife Disease Assoc.*, 4:37-40 (1968).

13. "Assessment of Experimental and Natural Viral Aerosols.", Gerone, P.J., et al., *Bacteriol. Rev.*, **30**: 576-584 (1966).

14. "The sampling efficiency of the thermal precipitator.", Watson, H. H., *Brit. J. Appl. Physics*, 2: 78-81 (1958).

15. "Non-Inertial Samplers: Biological Perspectives.", Crook, B., *Bioaerosols Handbook*, Chap 10 (1995).

References (cont.)

16. "Quantitative Characterization of Aerosols.", Wolfe, E. K., *Bacteriol. Rev.*, **25**, 194-202 (1961).

17. Mitchell, J. P. and W.D. Griffiths, *J. Aerosol Sci.*, Vol 21, pp. 392-395 (1990).

18. "Cyclone Collection Efficiency: Comparison of Experimental Results with Theoretical Predictions.", Dirgo, J. and D. Leith, *Aerosol Sci. and Technol.*, Vol 4: 401-415 (1985).

19. "Experimental Study of Particle Collection by Small Cyclones.", Kim, J. C., and K. W. Lee, *Aerosol Sci. and Technol.*, Vol 12: 1003-1015 (1990).

20. "Effect of Cyclone Dimensions on Gas Flow Pattern and Collection Efficiency.", Iozia, D. L. and D. Leith, *Aerosol Sci. and Technol.*, Vol 10: 491-500 (1989).

21. "Particle Collection Efficiencies of Air Sampling Cyclones: an Empirical Theory.", Chan, T. and M. Lippmann, *Environ. Sci. Technol.*, Vol. 11, No. 4, pp. 377-382 (1977).

22. "Air Pollution Control: A Design Approach.", Cooper, D. C., and Alley, F.C., Chapter 5, pp. 151-179 (1994).

23. "Electrostatic precipitation.", Masuda, S. and S. Hosokawa, *Handbook of Electrostatic Processes*, Chap 21 (1995).

24. Tagg, N.T., Personal communication (unpublished experiments), SRI International (1996).

Appendixes

Appendix A.

Variables used in Table 1.

N_{sf} = flow-line separation number [dimensionless]

D_p = particle diameter [L]

D_b = characteristic dimension of the collecting body [L]

N_{st} = inertial separation number [dimensionless]

K_m = Stokes-Cunningham correction factor [dimensionless]

$$= \frac{1}{1 + 2.1\left(D_p / D_b\right)}$$

ρ_p = particle density [M/L^3]

V_o = characteristic fluid velocity in the equipment [L/t]

μ = fluid viscosity [M/Lt]

N_{sd} = diffusional separation number [dimensionless]

D_v = particle diffusion coefficient [L^2/t]

$$= \frac{kT}{3\pi\mu D}$$ (Stoke's-Einstein Equation)

u_t = free settling velocity of particle due to gravity (terminal Stoke's velocity)[L/t]

$$= \frac{D_p^2\left(\rho_p - \rho\right)g}{18\mu}$$

N_{sg} = gravitational separation number [dimensionless]

N_{sec} = electrostatic-attraction separation number [dimensionless]

N_{sei} = electrostatic-induction separation number [dimensionless]

Q_p = electrical charge on particle [Coulombs]

ε_b =characteristic potential gradient at collecting surface [dynes/Coulomb]

δp = dielectric constant of particle [dimensionless]

δ_o = permittivity of free space [$Coloumbs^2$/dyne cm^2]

N_{st} = thermal separation number [dimensionless]

T = absolute characteristic fluid temperature [T]

T_b = absolute characteristic collecting body temperature [T]

ρ = fluid density [M/L^3]

k_t = thermal conductivity of the fluid [ML/t^3T]

k_{tp} = thermal conductivity of the particle [ML/t^3T]

g = acceleration due to gravity [ML/t^2]

Appendix B.

Results of a Comparison: 10-mm Cyclone and a Comparably Sized ESP.

Sampler	Particle Diameter (μm)	Efficiency	RequiredFlow Rate (lpm)	Sampling Time (min)
10-mm cyclone	1	0.9	18.5	0.6
Electrostatic precipitator	1	0.9	4.4	2.5

Correlations And Data Used In Comparison

I. Cyclone Correlation (Chan and Lippmann, 1977):

$$\eta = 0.5 + 0.5\tanh\left[B\left(\frac{D_p}{KQ^n}\right)^2 + (A-2B)\frac{D_p}{KQ^n} + B - A\right]$$

II. ESP Correlation (Masuda and Hosokawa, 1995):

$$\eta = 1 - \exp\left(-W_e f\right)^k$$

Parameter	Variable	Value	Parameter	Variable	Value
efficiency	η	0.9	efficiency	η	0.9
particle diameter	D_p	1 μm	empirical constant	k	0.5
volumetric flow	Q	calculate	effective migration	W_e	0.085
empirical constant	K	178.52	specific collection area	f	calculated
empirical constant	n	-2.13	collection area		40 cm²
empirical constant	A	0.74			
empirical constant	B	-0.07			
collection area		40 cm²			

Appendix C.

Method for determining mass median diameter and GSD using a weighted curve fit.

As described in USP guidelines (Seventh Supplement, p. 3126) a weighted least squares fit can sometimes be used to get the best fit while classifying particle size data. In this case, a weighted least squares regression fit to the log-probability relationship reduced to a two parameter equation (Selby, 1973) was used, given by Eq. (1):

$$D = \alpha \sigma_g^x \qquad (1)$$

D = particle diameter (μm)
α = mass median aerodynamic diameter (MMAD)
σ_g = geometric standard deviation (GSD)
x = the inverse of the standard normal cumulative distribution

In order to perform a least squares analysis, this equation is transformed into Eq.(2) by taking the logarithm of both sides, and solving for the variable x.

$$x = \frac{\ln\left(\frac{D}{\alpha}\right)}{\ln(\sigma_g)} \qquad (2)$$

The weighted least-squares error for a given set of N data points is a function of both the MMAD and the GSD, and is given by Eq. (3):

$$E = \sum_{i=1}^{N} \left(\frac{x_i - \ln\left(\frac{D_i}{\alpha}\right) \cdot \left(\ln(\sigma_g)\right)^{-1}}{\omega_i} \right)^2 \qquad (3)$$

ω_i = weight value for data point i

The partial derivatives of (3) with respect to both MMAD and GSD are given in Eq. (4) and (5).

$$0 = \frac{\partial E}{\partial \alpha} = \sum_{i=1}^{N} \left[\left(x_i - \ln\left(\frac{D_i}{\alpha}\right) \cdot \left(\ln(\sigma_g)\right)^{-1} \right) \cdot \left(\frac{\left(\ln(\sigma_g)\right)^{-1}}{\alpha \cdot \omega_i} \right) \right] \qquad (4)$$

$$0 = \frac{\partial E}{\partial \sigma_g} = \sum_{i=1}^{N} \left[\frac{\left(x_i - \ln\left(\frac{D_i}{\alpha}\right) \cdot \left(\ln(\sigma_g)\right)^{-1} \right) \cdot \left(\ln\left(\frac{D_i}{\alpha}\right) \right)}{\omega_i^2} \right] \tag{5}$$

Rearranging Eq.(4) and (5) gives expressions for ln(MMAD) and ln(GSD).

$$\ln(\alpha) = \frac{\sum_{i=1}^{N} \frac{\ln(x_i)}{\omega_i^2} - \ln(\sigma_g) \cdot \sum_{i=1}^{N} \frac{D_i}{\omega_i^2}}{\sum_{i=1}^{N} \frac{1}{\omega_i^2}} \tag{6}$$

$$\ln(\sigma_g) = \frac{\sum_{i=1}^{N} \left(\frac{\ln\left(\frac{D_i}{\alpha}\right)}{\omega_i} \right)^2}{\sum_{i=1}^{N} \frac{\ln\left(\frac{D_i}{\alpha}\right) \cdot x_i}{\omega_i^2}} \tag{7}$$

Eq. (6) and (7) are linear equations. Because of the complexity of the expressions, it is easiest to solve these using the iteration feature of Microsoft Excel, or some other computer algorithm.

Appendix D.

Tables of Experimental Data

Appendix D-1.

Cyclone Data and Material Balance

Variables used in data tables

V_{ni} = initial volume in nebulizer
N_I = initial weight of nebulizer
T_I = initial weight of tee
N_f = final weight of nebulizer
T_f = final weight of tee
Abs_n = absorbance measurement of neb solution
$C_{ni,f}$ = initial, final concentration in nebulizer
V_{nf} = volume remain in nebulizer
V_{tf} = volume remaining in tee
V_{fs} = volume sample fed to sampler
V_{ev} = volume of evaporation in neb
M_{vf} = final weight of collection vial
M_{vi} = initial weight of collection vial
V_{ci} = initial volume of rinse solution for cyclone
Abs_c = absorbance measurement for cyclone rinse
C_{ci} = initial concentration of cyclone solution
C_{cf} = final concentration of cyclone rinse solution
V_{fuv} = final rinse volume as determined by UV
V_c = volume left in cyclone
V_v = volume collected in vial
V_{tc} = total volume collected
V_{ei} = initial volume of rinse solution for ESP
Abs_e = absorbance measurement for ESP rinse
C_{ei} = initial concentration of ESP solution
C_{ef} = final concentration of ESP rinse solution
V_{esp} = volume left in ESP

Appendix D-1.

Cyclone Data and Material Balance (cont.)

RUN ID	V_{Ni} (ml)	N_i (g)	T_i (g)	N_f (g)	T_f (g)	Abs_N (AU)	CNi (mg/ml)	CNf (mg/ml)
1-C-B-5	4.0	12.9261	20.6720	11.2191	20.9180	3.4967	0.00478	0.00493
2-C-B-5	4.0	13.0515	20.7098	11.3933	21.0150	3.5205	0.00478	0.00499
3-C-B-5	4.0	13.1499	20.6765	11.4935	21.0437	3.4909	0.00478	0.00491
1-C-B-15	4.0	12.9646	20.7137	10.8121	21.2610	3.5269	0.00478	0.00500
2-C-B-15	4.0	13.0390	20.6546	10.3878	21.7566	3.5061	0.00478	0.00495
3-C-B-15	4.0	12.8799	20.7015	9.8546	22.0440	3.4486	0.00478	0.00480
1-C-B-25	4.0	12.9034	20.6757	9.7627	22.3928	3.5780	0.00478	0.00513
2-C-B-25	4.0	12.9531	20.6705	10.7632	21.5180	3.5166	0.00478	0.00498
3-C-B-25	4.0	12.9972	20.6779	9.6022	22.6071	3.5273	0.00478	0.00500

RUN ID	VNf (ml)	VTf (ml)	VFS (ml)	Vev (ml)	MVi (mg)	MVf (mg)	VCi (ml)	AbsC (AU)
1-C-B-5	2.29729	0.24538	1.45733	0.09723	1109.3	1453.2	2.0	0.87525
2-C-B-5	2.34597	0.30443	1.34960	0.13956	1108.7	1440.7	2.0	0.85398
3-C-B-5	2.34776	0.36628	1.28596	0.09018	1096.2	1354.3	2.0	0.82995
1-C-B-15	1.85291	0.54592	1.60117	0.14359	1104.1	1376.5	2.0	0.84756
2-C-B-15	1.35547	1.09923	1.54530	0.11114	1103.1	1315.5	2.0	0.85534
3-C-B-15	0.98230	1.33913	1.67857	0.01495	1104.9	1350.0	2.0	0.84698
1-C-B-25	0.86719	1.71278	1.42002	0.23234	1097.5	1397.7	2.0	0.89102
2-C-B-25	1.81560	0.84537	1.33903	0.13322	1104.7	1208.7	2.0	0.87987
3-C-B-25	0.61353	1.92435	1.46212	0.14802	1096.7	1299.2	2.0	0.89124

RUN ID	CCi (mg/ml)	CCf (mg/ml)	Vfuv (ml)	Vc (ml)	Vv (ml)	Vtc (ml)
1-C-B-5	0.02782	0.02517	2.21048	0.21048	0.3430	0.5535
2-C-B-5	0.02782	0.02457	2.26485	0.26485	0.3312	0.5960
3-C-B-5	0.02782	0.02389	2.32959	0.32959	0.2575	0.5870
1-C-B-15	0.02782	0.02439	2.28179	0.28179	0.2717	0.5535
2-C-B-15	0.02782	0.02461	2.26130	0.26130	0.2119	0.4732
3-C-B-15	0.02782	0.02437	2.28334	0.28334	0.2445	0.5278
1-C-B-25	0.02782	0.02562	2.17183	0.17183	0.2994	0.4713
2-C-B-25	0.02782	0.02530	2.19902	0.19902	0.1037	0.3028
3-C-B-25	0.02782	0.02563	2.17130	0.17130	0.2020	0.3733

Appendix D-1.

Cyclone Data and Material Balance (cont.)

RUN ID	Vni (ml)	% Total	Vnf (ml)	% Total	Vtf (ml)	% Total	Vev (ml)	% Total
1-C-B-5	4	100.0%	2.2973	57.4%	0.2454	6.1%	0.0972	2.4%
2-C-B-5	4	100.0%	2.3460	58.6%	0.3044	7.6%	0.1396	3.5%
3-C-B-5	4	100.0%	2.3478	58.7%	0.3663	9.2%	0.0902	2.3%
1-C-B-15	4	100.0%	1.8529	46.3%	0.5459	13.6%	0.1436	3.6%
2-C-B-15	4	100.0%	1.3555	33.9%	1.0992	27.5%	0.1111	2.8%
3-C-B-15	4	100.0%	0.9823	24.6%	1.3391	33.5%	0.0150	0.4%
1-C-B-25	4	100.0%	0.8672	21.7%	1.7128	42.8%	0.2323	5.8%
2-C-B-25	4	100.0%	1.8156	45.4%	0.8454	21.1%	0.1332	3.3%
3-C-B-25	4	100.0%	0.6135	15.3%	1.9244	48.1%	0.1480	3.7%

RUN ID	Vc (ml)	% Total	Vv (ml)	% Total	Acounted	Vtc (ml)	Vfs (ml)	Eff.
1-C-B-5	0.2105	5.3%	0.3430	8.6%	79.8%	0.5535	1.4573	38.0%
2-C-B-5	0.2649	6.6%	0.3312	8.3%	84.6%	0.5960	1.3496	44.2%
3-C-B-5	0.3296	8.2%	0.2575	6.4%	84.8%	0.5870	1.2860	45.6%
1-C-B-15	0.2818	7.0%	0.2717	6.8%	77.4%	0.5535	1.6012	34.6%
2-C-B-15	0.2613	6.5%	0.2119	5.3%	76.0%	0.4732	1.5453	30.6%
3-C-B-15	0.2833	7.1%	0.2445	6.1%	71.6%	0.5278	1.6786	31.4%
1-C-B-25	0.1718	4.3%	0.2994	7.5%	82.1%	0.4713	1.4200	33.2%
2-C-B-25	0.1990	5.0%	0.1037	2.6%	77.4%	0.3028	1.3390	22.6%
3-C-B-25	0.1713	4.3%	0.2020	5.0%	76.5%	0.3733	1.4621	25.5%

RUN ID	V_{Ni} (ml)	N_i (g)	T_i (g)	N_f (g)	T_f (g)	Abs_N (AU)	CNi (mg/ml)	CNf (mg/ml)
1-C-S-5	4.0	12.9820	20.7548	9.8563	21.8464	0.1732	0.00473	0.00523
2-C-S-5	4.0	12.9591	20.6466	10.1527	21.0815	0.1627	0.00473	0.00493
3-C-S-5	4.0	13.0722	20.6483	10.5369	21.2146	0.1621	0.00473	0.00491
1-C-S-15	4.0	12.8716	20.6188	10.8141	21.4870	0.1633	0.00473	0.00495
2-C-S-15	4.0	12.9250	20.6601	10.7795	21.6844	0.1573	0.00473	0.00477
3-C-S-15	4.0	13.0314	20.7581	10.7317	21.7675	0.1583	0.00473	0.00480
1-C-S-25	4.0	12.7253	20.5907	10.1399	21.9544	0.1563	0.00473	0.00475
2-C-S-25	4.0	12.8459	20.6517	9.5257	22.3556	0.1683	0.00473	0.00509
3-C-S-25	4.0	13.0054	20.6920	9.7831	22.3187	0.1632	0.00473	0.00494

Appendix D-1.

Cyclone Data and Material Balance (cont.)

RUN ID	VNf (ml)	VTf (ml)	VFS (ml)	Vev (ml)	MVi (mg)	MVf (mg)	VCi (ml)	AbsC (AU)
1-C-S-5	0.87736	1.09053	2.03211	0.28821	1103.2	2020.0	2.0	0.89526
2-C-S-5	1.19635	0.43447	2.36918	0.11102	1107.5	2079.3	2.0	0.89021
3-C-S-5	1.46718	0.56575	1.96707	0.11204	1109.9	1982.5	2.0	0.90020
1-C-S-15	1.94451	0.86735	1.18814	0.15398	1111.3	1471.7	1.5	0.88901
2-C-S-15	1.85660	1.02330	1.12010	0.03487	1103.8	1335.0	2.0	0.89287
3-C-S-15	1.70259	1.00841	1.28900	0.05355	1099	1394.2	2.0	0.90544
1-C-S-25	1.41713	1.36236	1.22050	0.01556	1104.6	1403.5	2.0	0.90176
2-C-S-25	0.68305	1.70223	1.61472	0.23101	1110.9	1379.2	2.0	0.88179
3-C-S-25	0.78085	1.62511	1.59404	0.14153	1103.1	1384.7	2.0	0.91245

RUN ID	CCi (mg/ml)	CCf (mg/ml)	Vfuv (ml)	Vc (ml)	Vv (ml)	Vtc (ml)
1-C-S-5	0.02782	0.02574	2.16167	0.16167	0.9159	1.0776
2-C-S-5	0.02782	0.0256	2.17378	0.17378	0.9708	1.1446
3-C-S-5	0.02782	0.02588	2.14994	0.14994	0.8717	1.0217
1-C-S-15	0.02782	0.02556	1.63251	0.13251	0.3600	0.4926
2-C-S-15	0.02782	0.02567	2.16738	0.16738	0.2310	0.3984
3-C-S-15	0.02782	0.02603	2.13765	0.13765	0.2949	0.4326
1-C-S-25	0.02782	0.02593	2.14627	0.14627	0.2986	0.4449
2-C-S-25	0.02782	0.02536	2.19430	0.19430	0.2680	0.4623
3-C-S-25	0.02782	0.02623	2.12143	0.12143	0.2813	0.4028

RUN ID	Vni (ml)	% Total	Vnf (ml)	% Total	Vtf (ml)	% Total	Vev (ml)	% Total
1-C-S-5	4	100.0%	0.8774	21.9%	1.0905	27.3%	0.2882	7.2%
2-C-S-5	4	100.0%	1.1963	29.9%	0.4345	10.9%	0.1110	2.8%
3-C-S-5	4	100.0%	1.4672	36.7%	0.5657	14.1%	0.1120	2.8%
1-C-S-15	4	100.0%	1.9445	48.6%	0.8673	21.7%	0.1540	3.8%
2-C-S-15	4	100.0%	1.8566	46.4%	1.0233	25.6%	0.0349	0.9%
3-C-S-15	4	100.0%	1.7026	42.6%	1.0084	25.2%	0.0535	1.3%
1-C-S-25	4	100.0%	1.4171	35.4%	1.3624	34.1%	0.0156	0.4%
2-C-S-25	4	100.0%	0.6831	17.1%	1.7022	42.6%	0.2310	5.8%
3-C-S-25	4	100.0%	0.7809	19.5%	1.6251	40.6%	0.1415	3.5%

Appendix D-1.

Cyclone Data and Material Balance (cont.)

RUN ID	Vc (ml)	% Total	Vv (ml)	% Total	Acounted	Vtc (ml)	Vfs (ml)	Eff.
1-C-S-5	0.1617	4.0%	0.9159	22.9%	83.3%	1.0776	2.0321	53.0%
2-C-S-5	0.1738	4.3%	0.9708	24.3%	72.2%	1.1446	2.3692	48.3%
3-C-S-5	0.1499	3.7%	0.8717	21.8%	79.2%	1.0217	1.9671	51.9%
1-C-S-15	0.1325	3.3%	0.3600	9.0%	86.5%	0.4926	1.1881	41.5%
2-C-S-15	0.1674	4.2%	0.2310	5.8%	82.8%	0.3984	1.1201	35.6%
3-C-S-15	0.1376	3.4%	0.2949	7.4%	79.9%	0.4326	1.2890	33.6%
1-C-S-25	0.1463	3.7%	0.2986	7.5%	81.0%	0.4449	1.2205	36.5%
2-C-S-25	0.1943	4.9%	0.2680	6.7%	77.0%	0.4623	1.6147	28.6%
3-C-S-25	0.1214	3.0%	0.2813	7.0%	73.8%	0.4028	1.5940	25.3%

Summary: Average cyclone physical efficiency data.

Run s	Organism	Flow Rate (lpm)	Average Efficiency (%)
1,2,-3-C-B-5	*B. subtilis*	5	43% ± 4%
1,2,-3-C-B-15	*B. subtilis*	15	32% ± 2%
1,2,-3-C-B-25	*B. subtilis*	25	27% ± 6%
1,2,-3-C-S-5	*S. marcescens*	5	51% ± 3%
1,2,-3-C-S-15	*S. marcescens*	15	37% ± 4%
1,2,-3-C-S-25	*S. marcescens*	25	30% ± 6%

Appendix D-2.

Electrostatic Precipitator Data and Material Balance

RUN ID	V_{Ni} (ml)	N_i (g)	T_i (g)	N_f (g)	T_f (g)	Abs_N (AU)	CNi (mg/ml)	CNf (mg/ml)
1-E-B-5	4.0	13.0131	20.6824	11.7540	20.8671	3.4779	0.00478	0.00488
2-E-B-5	4.0	12.8791	20.7795	11.5791	21.1237	3.4959	0.00478	0.00492
3-E-B-5	4.0	13.0111	20.7074	11.4686	21.3325	3.4582	0.00478	0.00483
1-E-B-15	4.0	13.0328	20.6744	11.5402	21.4559	3.4848	0.00478	0.00490
2-E-B-15	4.0	13.0253	20.6783	11.3010	21.6432	3.4800	0.00478	0.00488
3-E-B-15	4.0	12.9992	20.7801	11.3948	21.2141	3.5189	0.00478	0.00498
1-E-B-25	4.0	12.9609	20.6471	10.3491	22.5841	3.5067	0.00478	0.00495
2-E-B-25	4.0	12.8655	20.6887	11.2331	21.4658	3.5697	0.00478	0.00511
3-E-B-25	4.0	12.9003	20.6693	11.0510	21.6802	3.5793	0.00478	0.00514

RUN ID	VNf (ml)	VTf (ml)	VFS (ml)	Vev (ml)	MVi (mg)	MVf (mg)	Vei (ml)	Abse (AU)
1-E-B-5	2.74406	0.18424	1.07170	0.06998	1096.6	1611.8	2.0	0.86912
2-E-B-5	2.70332	0.34333	0.95335	0.10443	1097.6	1642.7	2.0	0.87974
3-E-B-5	2.46138	0.62353	0.91509	0.03504	1105.3	1608.7	2.0	0.87900
1-E-B-15	2.51113	0.77954	0.70933	0.08722	1103.6	1423.5	1.0	0.78090
2-E-B-15	2.28001	0.96247	0.75752	0.07747	1097.7	1439.4	2.0	0.87025
3-E-B-15	2.39966	0.43291	1.16743	0.14119	1098.6	1493.0	2.0	0.81765
1-E-B-25	1.39478	1.93213	0.67309	0.12942	1109.9	1358.3	2.0	0.85945
2-E-B-25	2.37170	0.77515	0.85316	0.24037	1110.7	1398.9	2.0	0.84242
3-E-B-25	2.15536	1.00836	0.83628	0.25814	1105.1	1318.7	2.0	0.83308

RUN ID	Cei (mg/ml)	Cef (mg/ml)	Vfuv (ml)	Vesp (ml)	Vv (ml)	Vtc (ml)
1-E-B-5	0.02782	0.025	2.22588	0.22588	0.5139	0.7398
2-E-B-5	0.02782	0.0253	2.19934	0.19934	0.5437	0.7431
3-E-B-5	0.02782	0.02528	2.20116	0.20116	0.5021	0.7033
1-E-B-15	0.02782	0.02249	1.23696	0.23696	0.3191	0.5561
2-E-B-15	0.02782	0.02503	2.22302	0.22302	0.3408	0.5639
3-E-B-15	0.02782	0.02354	2.36417	0.36417	0.3934	0.7576
1-E-B-25	0.02782	0.02472	2.25062	0.25062	0.2478	0.4984
2-E-B-25	0.02782	0.02424	2.29555	0.29555	0.2875	0.5830
3-E-B-25	0.02782	0.02397	2.32095	0.32095	0.2131	0.5340

Appendix D-2.

Electrostatic Precipitator Data and Material Balance (cont.)

RUN ID	Vni (ml)	% Total	Vnf (ml)	% Total	Vtf (ml)	% Total	Vev (ml)	% Total
1-E-B-5	4	100.0%	2.7441	68.6%	0.1842	4.6%	0.0700	1.7%
2-E-B-5	4	100.0%	2.7033	67.6%	0.3433	8.6%	0.1044	2.6%
3-E-B-5	4	100.0%	2.4614	61.5%	0.6235	15.6%	0.0350	0.9%
1-E-B-15	4	100.0%	2.5111	62.8%	0.7795	19.5%	0.0872	2.2%
2-E-B-15	4	100.0%	2.2800	57.0%	0.9625	24.1%	0.0775	1.9%
3-E-B-15	4	100.0%	2.3997	60.0%	0.4329	10.8%	0.1412	3.5%
1-E-B-25	4	100.0%	1.3948	34.9%	1.9321	48.3%	0.1294	3.2%
2-E-B-25	4	100.0%	2.3717	59.3%	0.7751	19.4%	0.2404	6.0%
3-E-B-25	4	100.0%	2.1554	53.9%	1.0084	25.2%	0.2581	6.5%

RUN ID	Vesp (ml)	% Total	Vv (ml)	% Total	Acounted	Vtc (ml)	Vfs (ml)	Eff.
1-E-B-5	0.2259	5.6%	0.5139	12.8%	93.5%	0.7398	1.0717	69.0%
2-E-B-5	0.1993	5.0%	0.5437	13.6%	97.4%	0.7431	0.9533	77.9%
3-E-B-5	0.2012	5.0%	0.5021	12.6%	95.6%	0.7033	0.9151	76.9%
1-E-B-15	0.2370	5.9%	0.3191	8.0%	98.3%	0.5561	0.7093	78.4%
2-E-B-15	0.2230	5.6%	0.3408	8.5%	97.1%	0.5639	0.7575	74.4%
3-E-B-15	0.3642	9.1%	0.3934	9.8%	93.3%	0.7576	1.1674	64.9%
1-E-B-25	0.2506	6.3%	0.2478	6.2%	98.9%	0.4984	0.6731	74.0%
2-E-B-25	0.2956	7.4%	0.2875	7.2%	99.3%	0.5830	0.8532	68.3%
3-E-B-25	0.3209	8.0%	0.2131	5.3%	98.9%	0.5340	0.8363	63.9%

RUN ID	V_{Ni} (ml)	N_i (g)	T_i (g)	N_f (g)	T_f (g)	Abs_N (AU)	CNi (mg/ml)	CNf (mg/ml)
1-E-S-5	4.0	12.9889	20.6788	11.5227	21.2835	0.1613	0.00473	0.00489
2-E-S-5	4.0	13.0236	20.6719	11.9822	20.8834	0.1606	0.00473	0.00487
3-E-S-5	4.0	13.0244	20.7221	11.5472	21.2245	0.1638	0.00473	0.00496
1-E-S-15	4.0	13.1978	20.6725	11.5541	21.5014	0.1620	0.00473	0.00491
2-E-S-15	4.0	12.9046	20.0699	10.9709	21.1723	0.1620	0.00473	0.00491
3-E-S-15	4.0	12.9129	20.4752	9.3785	23.2131	0.1653	0.00473	0.00500
1-E-S-25	4.0	12.9804	20.7027	11.0237	21.8099	0.1638	0.00473	0.00496
2-E-S-25	4.0	13.0203	20.7190	11.1352	21.6478	0.1656	0.00473	0.00501
3-E-S-25	4.0	13.0182	20.6705	11.1318	21.7073	0.1614	0.00473	0.00489

Appendix D-2.

Electrostatic Precipitator Data and Material Balance (cont.)

RUN ID	VNf (ml)	VTf (ml)	VFS (ml)	Vev (ml)	MVi (mg)	MVf (mg)	Vei (ml)	Abse (AU)
1-E-S-5	2.53524	0.60411	0.86066	0.12008	1097.4	1484.0	2.0	0.86747
2-E-S-5	2.95965	0.21129	0.82906	0.10714	1094.1	1463.7	2.0	0.88914
3-E-S-5	2.52428	0.50191	0.97381	0.16993	1096	1570.6	2.0	0.87909
1-E-S-15	2.35791	0.82809	0.81400	0.13645	1108.6	1491.1	2.0	0.88356
2-E-S-15	2.06818	1.10135	0.83047	0.13542	1097.4	1480.6	2.0	0.86374
3-E-S-15	0.46906	2.73522	0.79572	0.20389	1096.8	1453.3	2.0	0.88907
1-E-S-25	2.04522	1.10612	0.84866	0.17179	1104.9	1385.9	2.0	0.83900
2-E-S-25	2.11673	0.92789	0.95538	0.20519	1096.1	1395.9	2.0	0.84891
3-E-S-25	2.11542	1.03578	0.84880	0.12330	1106.1	1384.0	2.0	0.83936

RUN ID	Cei (mg/ml)	Cef (mg/ml)	Vfuv (ml)	Vesp (ml)	Vv (ml)	Vtc (ml)
1-E-S-5	0.02782	0.02495	2.23007	0.23007	0.3862	0.6163
2-E-S-5	0.02782	0.02557	2.17637	0.17637	0.3692	0.5456
3-E-S-5	0.02782	0.02528	2.20095	0.20095	0.4741	0.6751
1-E-S-15	0.02782	0.02541	2.18994	0.18994	0.3821	0.5721
2-E-S-15	0.02782	0.02485	2.23958	0.23958	0.3828	0.6224
3-E-S-15	0.02782	0.02557	2.17653	0.17653	0.3562	0.5327
1-E-S-25	0.02782	0.02414	2.30477	0.30477	0.2807	0.5855
2-E-S-25	0.02782	0.02442	2.27820	0.27820	0.2995	0.5777
3-E-S-25	0.02782	0.02415	2.30380	0.30380	0.2776	0.5814

RUN ID	Vni (ml)	% Total	Vnf (ml)	% Total	Vtf (ml)	% Total	Vev (ml)	% Total
1-E-S-5	4	100.0%	2.5352	63.4%	0.6041	15.1%	0.1201	3.0%
2-E-S-5	4	100.0%	2.9596	74.0%	0.2113	5.3%	0.1071	2.7%
3-E-S-5	4	100.0%	2.5243	63.1%	0.5019	12.5%	0.1699	4.2%
1-E-S-15	4	100.0%	2.3579	58.9%	0.8281	20.7%	0.1364	3.4%
2-E-S-15	4	100.0%	2.0682	51.7%	1.1014	27.5%	0.1354	3.4%
3-E-S-15	4	100.0%	0.4691	11.7%	2.7352	68.4%	0.2039	5.1%
1-E-S-25	4	100.0%	2.0452	51.1%	1.1061	27.7%	0.1718	4.3%
2-E-S-25	4	100.0%	2.1167	52.9%	0.9279	23.2%	0.2052	5.1%
3-E-S-25	4	100.0%	2.1154	52.9%	1.0358	25.9%	0.1233	3.1%

Appendix D-2.

Electrostatic Precipitator Data and Material Balance (cont.)

RUN ID	Vesp (ml)	% Total	Vv (ml)	% Total	Acounted	Vtc (ml)	Vfs (ml)	Eff.
1-E-S-5	0.2301	5.8%	0.3862	9.7%	96.9%	0.6163	0.8607	71.6%
2-E-S-5	0.1764	4.4%	0.3692	9.2%	95.6%	0.5456	0.8291	65.8%
3-E-S-5	0.2010	5.0%	0.4741	11.9%	96.8%	0.6751	0.9738	69.3%
1-E-S-15	0.1899	4.7%	0.3821	9.6%	97.4%	0.5721	0.8140	70.3%
2-E-S-15	0.2396	6.0%	0.3828	9.6%	98.2%	0.6224	0.8305	74.9%
3-E-S-15	0.1765	4.4%	0.3562	8.9%	98.5%	0.5327	0.7957	66.9%
1-E-S-25	0.3048	7.6%	0.2807	7.0%	97.7%	0.5855	0.8487	69.0%
2-E-S-25	0.2782	7.0%	0.2995	7.5%	95.7%	0.5777	0.9554	60.5%
3-E-S-25	0.3038	7.6%	0.2776	6.9%	96.4%	0.5814	0.8488	68.5%

Summary: Average electrostatic precipitator physical efficiency data.

Run s	Organism	Flow Rate (lpm)	Average Efficiency (%)
1,2,-3-E-B-5	B. subtilis	5	75% ± 5%
1,2,-3-E-B-15	B. subtilis	15	73% ± 7%
1,2,-3-E-B-25	B. subtilis	25	69% ± 5%
1,2,-3-E-S-5	S. marcescens	5	69% ± 3%
1,2,-3-E-S-15	S. marcescens	15	71% ± 4%
1,2,-3-E-S-25	S. marcescens	25	66% ± 5%

Appendix D-3.

Cyclone Bioefficiency Data

RUN ID	Initial Cell Count (cells/ml)	Final Cell Count (cells/ml)	Efficiency	Initial CFU	Final CFU	Bio-efficiency
1-C-B-5	1.10E+07	not detectable	NA	1.10E+06	7.10E+04	6%
2-C-B-5	1.10E+07	not detectable	NA	1.10E+06	4.50E+04	4%
3-C-B-5	1.10E+07	not detectable	NA	1.10E+06	6.00E+04	5%
1-C-B-15	1.10E+07	1.10E+07	100%	1.10E+06	1.50E+06	100%
2-C-B-15	1.10E+07	7.10E+06	65%	1.10E+06	7.50E+05	68%
3-C-B-15	1.10E+07	9.20E+06	84%	1.10E+06	1.30E+06	100%
1-C-B-25	1.10E+07	not detectable	NA	1.10E+06	9.40E+04	9%
2-C-B-25	1.10E+07	not detectable	NA	1.10E+06	3.50E+05	32%
3-C-B-25	1.10E+07	not detectable	NA	1.10E+06	6.00E+04	5%
1-C-S-5	6.90E+06	6.10E+06	88%	5.20E+06	3.00E+06	58%
2-C-S-5	6.90E+06	3.40E+06	49%	5.20E+06	6.00E+06	100%
3-C-S-5	6.90E+06	4.20E+06	61%	5.20E+06	2.50E+06	48%
1-C-S-15	1.60E+07	1.50E+07	94%	5.20E+06	4.00E+06	77%
2-C-S-15	1.60E+07	1.60E+07	100%	5.20E+06	8.00E+06	100%
3-C-S-15	1.60E+07	1.50E+07	94%	5.20E+06	4.50E+06	87%
1-C-S-25	6.90E+06	5.00E+06	72%	5.20E+06	6.00E+06	100%
2-C-S-25	6.90E+06	5.90E+06	86%	5.20E+06	6.60E+06	100%
3-C-S-25	6.90E+06	3.70E+06	54%	5.20E+06	8.00E+06	100%

Summary: Average cyclone bioefficiency data.

Run s	Organism	Flow Rate (lpm)	Avg. Transfer Eff. (%)	Average Bioefficiency (%)
1,2,-3-C-B-5	*B. subtilis*	5	no detection	5% ± 1
1,2,-3-C-B-15	*B. subtilis*	15	83% ± 18%	89% ± 18%
1,2,-3-C-B-25	*B. subtilis*	25	no detection	15% ± 14%
1,2,-3-C-S-5	*S. marcescens*	5	66% ± 20%	69% ± 28%
1,2,-3-C-S-15	*S. marcescens*	15	96% ± 4%	96% ± 12%
1,2,-3-C-S-25	*S. marcescens*	25	71% ± 16 %	100% ± 0%

Appendix D-4.

ESP Bioefficiency Data

RUN ID	Initial Cell Count (cells/ml)	Final Cell Count (cells/ml)	Efficiency	Initial CFU	Final CFU	Bio-efficiency
1-E-B-5	9.10E+06	2.50E+06	27%	9.70E+05	1.30E+05	13%
2-E-B-5	9.10E+06	3.80E+06	42%	9.70E+05	7.00E+04	7%
3-E-B-5	9.10E+06	4.00E+06	44%	9.70E+05	1.30E+05	13%
1-E-B-15	9.10E+06	1.20E+07	100%	9.70E+05	1.20E+06	100%
2-E-B-15	9.10E+06	8.00E+06	88%	9.70E+05	9.50E+05	98%
3-E-B-15	9.10E+06	7.40E+06	81%	9.70E+05	1.40E+06	100%
1-E-B-25	9.10E+06	6.50E+06	71%	9.70E+05	5.60E+05	58%
2-E-B-25	9.10E+06	7.90E+06	87%	9.70E+05	1.10E+06	100%
3-E-B-25	9.10E+06	7.20E+06	79%	9.70E+05	7.00E+05	72%
1-E-S-5	6.80E+06	9.30E+06	100%	9.00E+06	7.00E+06	78%
2-E-S-5	1.00E+07	6.60E+06	66%	9.00E+06	1.00E+07	100%
3-E-S-5	8.80E+06	6.20E+06	70%	9.00E+06	7.00E+06	78%
1-E-S-15	1.50E+07	1.60E+07	100%	9.00E+06	9.00E+06	100%
2-E-S-15	1.50E+07	1.60E+07	100%	9.00E+06	1.00E+07	100%
3-E-S-15	1.50E+07	1.50E+07	100%	9.00E+06	9.00E+06	100%
1-E-S-25	1.50E+07	1.20E+07	80%	9.00E+06	8.00E+06	89%
2-E-S-25	1.10E+07	8.20E+06	75%	9.00E+06	8.50E+06	94%
3-E-S-25	8.20E+06	9.50E+06	100%	9.00E+06	5.00E+06	56%

Summary: Average ESP bioefficiency data.

Run s	Organism	Flow Rate (lpm)	Avg. Transfer Eff. (%)	Average Bioefficiency (%)
1,2,-3-E-B-5	*B. subtilis*	5	38% ± 9%	11% ± 4
1,2,-3-E-B-15	*B. subtilis*	15	90% ± 9%	99% ± 1%
1,2,-3-E-B-25	*B. subtilis*	25	79% ± 8%	77% ± 21%
1,2,-3-E-S-5	*S. marcescens*	5	79% ± 18%	85% ± 13%
1,2,-3-E-S-15	*S. marcescens*	15	100% ± 0%	100% ± 0%
1,2,-3-E-S-25	*S. marcescens*	25	85% ± 13 %	80% ± 21%

Appendix D-5.

Power Requirement Data for the Cyclone and ESP

Sampler	Flow Rate (lpm)	Pressure Drop (in H_2O)	Power Requirement (W)*
Cyclone	5	3.9	0.08
Cyclone	15	43.1	2.68
Cyclone	25	90.0	9.33
ESP	5	1.0	0.41
ESP	15	8.0	0.89
ESP	25	18.0	2.26

***Includes electrical power for the ESP (195 V x 0.002 A = 0.39 W)**

Appendix E.

Plots of Experimental Data

Appendix E-1.

ONP Standard Curve.

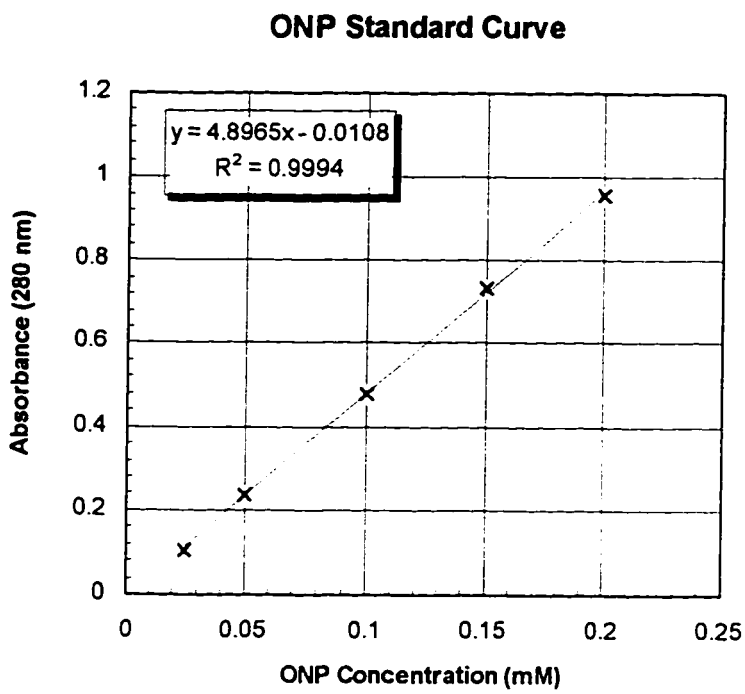

Appendix E-2.

Sample Malvern Output.

System number 2355 Diode ES977

Malvern Instruments EASY Particle Sizer M6.02 Date 06-01-94 Time 05-53

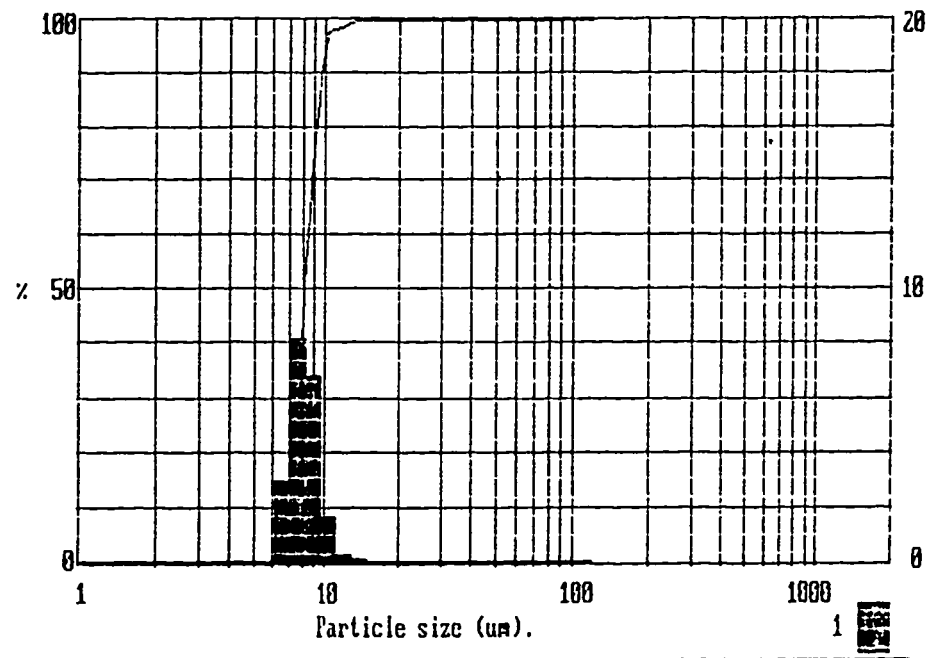

Size : microns	: under	% in band:	Size : microns	: under	% in band:
118.4	100.0	0.0	11.1	38.4	8.5
102.2	100.0	0.0	9.6	89.8	34.1
88.2	100.0	0.0	8.3	55.7	40.7
76.0	100.0	0.0	7.2	15.0	14.9
65.6	100.0	0.0	6.2	0.1	0.1
56.6	100.0	0.0	5.3	0.0	0.0
48.8	100.0	0.0	4.6	0.0	0.0
42.1	100.0	0.0	4.0	0.0	0.0
36.3	100.0	0.0	3.4	0.0	0.0
31.4	100.0	0.0	3.0	0.0	0.0
27.1	100.0	0.0	2.6	0.0	0.0
23.3	100.0	0.0	2.2	0.0	0.0
20.2	100.0	0.0	1.9	0.0	0.0
17.3	100.0	0.0	1.6	0.0	0.0
15.0	100.0	0.3	1.4	0.0	0.0
12.9	99.7	1.3	1.2	0.0	

Result source= Sample
Record No. = 0
Focal length = 63 mm.
Experiment type lds
Volume distribution
Beam length = 20.0 mm.
Obscuration =-.2024
Volume Conc. = 0.0000 %
Log. Diff. =5.90
Model indp

D(v,0.5) = 8.1 um
D(v,0.9) = 9.6 um
D(v,0.1) = 7.0 um
D(4,3) = 8.2 um
D(3,2) = 8.1 um
Span = 0.3
Spec. surf. area
0.7387 sq.m./cc.